




RESEARCH PAPER



Identification of highly selective type II kinase inhibitors with chiral peptidomimetic tails

Seo-Jung Han^{a,b} , Jae Eun Jung^{a,c}, Do Hee Oh^{a,c}, Minsup Kim^d, Jae-Min Kim^{e,f}, Kyung-Sook Chung^e, Hee-Soo Han^{e,g}, Jeong-Hun Lee^{e,g}, Kyung-Tae Lee^{e,f}, Hee Jin Jeong^a, In Ho Park^{h,i} , Eunkyeong Jeon^{ij}, Jeon-Soo Shin^{h,ij} , Dongkeun Hwang^a, Art E. Cho^{d,k}, Duck-Hyung Lee^c and Taeho Sim^{a,h}

^aChemical Kinomics Research Center, Korea Institute of Science and Technology, Seoul, Republic of Korea; ^bDivision of Bio-Medical Science & Technology, KIST School, UST, Seoul, Republic of Korea; ^cDepartment of Chemistry, Sogang University, Seoul, Republic of Korea; ^dDrug Discovery Institute, inCerebro Co., Ltd., Seoul, Republic of Korea; ^eDepartment of Pharmaceutical Biochemistry, College of Pharmacy, Kyung Hee University, Seoul, Republic of Korea; ^fDepartment of Biomedical and Pharmaceutical Sciences, Graduate School, Kyung Hee University, Seoul, Republic of Korea; ^gDepartment of Life and Nanopharmaceutical Sciences, College of Pharmacy, Kyung Hee University, Seoul, Republic of Korea; ^hSeverance Biomedical Science Institute, Yonsei University College of Medicine, Seoul, Republic of Korea; ⁱInstitute of Immunology and Immunological Diseases, Yonsei University College of Medicine, Seoul, Republic of Korea; ^jDepartment of Microbiology, Yonsei University College of Medicine, Seoul, Republic of Korea; ^kDepartment of Bioinformatics, Korea University, Sejong, Republic of Korea

ABSTRACT

Identification of highly selective type II kinase inhibitors is described. Two different chiral peptidomimetic scaffolds were introduced on the tail region of non-selective type II kinase inhibitor GNF-7 to enhance the selectivity. Kinome-wide selectivity profiling analysis showed that type II kinase inhibitor **7a** potently inhibited Lck kinase with great selectivity (IC₅₀ of 23.0 nM). It was found that **7a** and its derivatives possessed high selectivity for Lck over even structurally conserved all Src family kinases. We also observed that **7a** inhibited Lck activation in Jurkat T cells. Moreover, **7a** was found to alleviate clinical symptoms in DSS-induced colitis mice. This study provides a novel insight into the design of selective type II kinase inhibitors by adopting chiral peptidomimetic moieties on the tail region.

ARTICLE HISTORY

Received 14 January 2022
Revised 2 April 2022
Accepted 12 April 2022

KEYWORDS



Type-II kinase; Lck; DSS-induced colitis


1. Introduction

Most signal transduction processes are mediated through a phosphotransfer reactions catalysed by kinases. However, overexpression or mutation of kinases causes tumour cell proliferation and survival. Therefore, kinases are pursued as invaluable targets and a tremendous amount of effort has been devoted towards the discovery of small molecular kinase inhibitors for the treatment of cancer for decades¹. Small molecule kinase inhibitors have been classified by binding modes with protein kinases. Type I inhibitors are the most commonly encountered and occupy the ATP-binding site of the active conformation of kinases (i.e. DFG-in conformation). In contrast to type I inhibitors, type II kinase inhibitors recognise the ATP-binding pocket of inactive DFG-out conformation of kinase proteins. Besides ATP competitive inhibitors (e.g. type I, type II), allosteric and covalent inhibitors have also been investigated^{1–4}. Although a significant number of small molecular kinase inhibitors have been developed, discovery of selective kinase inhibitors remains challenging. The rationale behind this is that the structure of ATP-binding site in all of the kinase proteins is highly conserved¹. In addition, designing an allosteric kinase inhibitor, which is the most selective inhibitor, is difficult since it highly relies on an empirical exercise^{2a}. Although selective kinases have been uncovered using subtle 3-dimensional structural differences among the kinases⁵, discovery of highly selective kinase

inhibitors still remains a largely unmet challenge. Type II kinase inhibitors were anticipated to be more selective compared to type I kinase inhibitors in the early phase since the hydrophobic pocket generated by the DFG-out conformation is not quite conserved in contrast to ATP binding pocket and DFG-out conformations are more dynamic. However, type II kinase inhibitors, developed to date have been proven to be largely less selective than type I kinase inhibitors.^{2a}

We noticed that a number of the less selective type II kinase inhibitors possess achiral and limited chemotype tails, which interact with allosteric site of the inactive conformation of kinases. We envisioned that interactions of flat and achiral tail fragments with 3-dimensional structural kinases would be highly limited and resulted in less selective profile⁶. Thus, we were curious whether type II kinase inhibitors containing chiral tails would be more selective among all of the kinases by affording various binding modes^{7,8}. We were particularly interested in peptidomimetic structure as tail scaffolds. To our best knowledge, development of selective type II kinase inhibitors that consists of peptidomimetic tails is unprecedented. To investigate how peptidomimetic tail structure affects kinase selectivities, we chose the core structure of GNF-7 (Figure 1)⁹. GNF-7 has been discovered as a type II T3151 Bcr-Abl kinase inhibitor and possesses remarkable potencies against many kinases with highly low kinase selectivity. Among

CONTACT Seo-Jung Han  sjhan@kist.re.kr  Chemical Kinomics Research Center, Korea Institute of Science and Technology, 5 Hwarang-ro 14-gil, Seongbuk-gu, Seoul 02792, Republic of Korea

 Supplemental data for this article can be accessed [here](#).

© 2022 The Author(s). Published by Informa UK Limited, trading as Taylor & Francis Group.

This is an Open Access article distributed under the terms of the Creative Commons Attribution License (<http://creativecommons.org/licenses/by/4.0/>), which permits unrestricted use, distribution, and reproduction in any medium, provided the original work is properly cited.

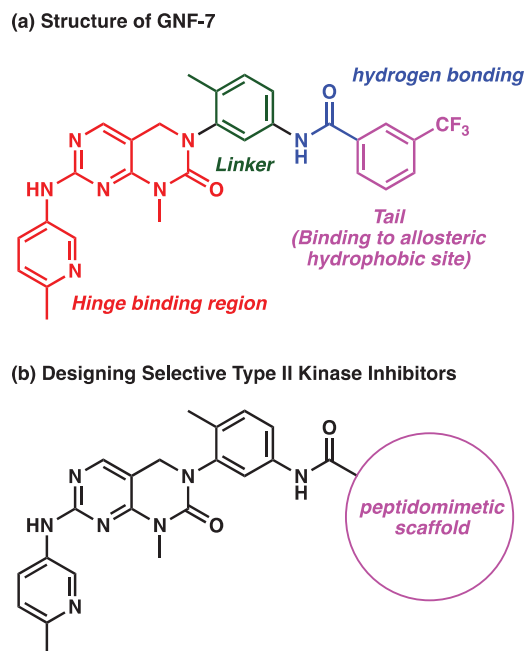


Figure 1. (a) Structure of GNF-7. (b) Designing selective type II kinase inhibitors with peptidomimetic scaffolds.

the peptidomimetic structure, we were attracted to synthetically easily accessible solution phase turn mimetic libraries¹⁰.

2. Results and discussion

2.1. Chemistry

We initially prepared kinase inhibitors, containing small molecular β -turn mimetic scaffolds developed by the Miller group (Scheme 1(a))^{10b,f}. Alkylation of chloromethyl pyrimidine **2** with aniline **1** provided *tert*-butyl ester **3** under basic conditions in 81% yield. Nucleophilic aromatic substitution of 2,4-dichloropyrimidine **3** with methylamine, followed by cyclic urea formation using triphosgene afforded urea **4**. Buchwald coupling of chloropyrimidine **4** with 5-aminopicoline and subsequent removal of *tert*-butyl group under acidic conditions smoothly generated acid **5**. Amide coupling of acid **5** with various β -turn mimetic scaffolds **6** produced amides **7** in 10–20% yields. We also prepared kinase inhibitors containing benzodiazepines as turn mimetic scaffolds (Scheme 1(b)). Amide coupling of benzodiazepines **9** and **10**^{10d,e} with aniline **8**^{9a,c} afforded amides **11** in 10–20% yields.

2.2. In vitro kinase inhibitory activities

Kinase-inhibitory activities of both **7** and **11** against four selected kinases were assessed by *in vitro* kinase assay (Table 1). To our delight, both **7a** and **11b** showed high degree of selectivities among selected kinases even between structurally similar Lck and c-Src (over 10-fold selectivities). Replacement of L-Pro with D-Pro led to lower selectivities between Lck and c-Src (**7a** and **7b**). This is not surprising since stereochemical alteration of Pro at *i*+1 might potentially change 3-dimensional conformation of the structure^{10b}. The substituents at N-1, C-3, and C-5 positions on the 1,4-benzodiazepin-2-one ring significantly affected selectivities. In all cases, the activities on Lck kinases were found to be superior to those on other kinases. Gratifyingly, **11b** possessed over 10-fold selectivity for Lck over c-Src. The *iso*-butyl group at C-3 position in the 1,4-benzodiazepin-2-one surpassed the methyl group in

respect of the selectivity (**11b** and **11d**). Also, the 2-butyl group at the C-3 position causes almost no selectivity (**11e**).

With the exciting initial data in hand, selectivities between Lck and c-Src were investigated on derivatives **7** containing the β -turn mimetic scaffolds (Table 2). Kinase-inhibitory activities of derivatives **7** against Lck and c-Src were assessed by *in vitro* kinase assay. Interestingly, **7c** possessing alternative stereochemistry compared to **7a** showed significantly (>10-fold) diminished selectivity. Changing *i*+2 functional groups to cyclopropane (**7d** and **7e**), cyclobutane (**7f**), and even glycine (**7g** and **7h**) exhibited high selectivities. However, we observed diminished selectivity with benzyl substitution at *i*+2 position (**7i**). High selectivity was kept with piperidine scaffold at *i*+1 (**7j**). In contrast to the pyrrolidine and the piperidine groups, addition of the azetidine at *i*+1 (**7k**) resulted in over 10-fold lower selectivity. The selectivities were not decreased by replacement of *iso*-butyl with valine at *i*+3 (**7l**, **7m**, **7n**, and **7o**). Substituents at *i* significantly affected selectivities (**7p**, **7q**, **7r**, **7s**, and **7t**). High selectivities were observed with *iso*-butyl and cyclohexyl substitution at *i* (over 10-fold selectivities, **7q** and **7s**). Compared to **7a**, The selectivities of **7v** and **7w** on Lck and c-Src were highly diminished^{10f}.

Additionally, we investigated the selectivities of derivatives containing benzodiazepine scaffolds on Lck and c-Src kinases (Table 3). Kinase-inhibitory activities of derivatives **11** against Lck and c-Src were assessed by *in vitro* kinase assay. The selectivities of **11f** was similar to those of its enantiomer **11a** and *p*-fluorobenzyl **11g**. It is noteworthy that the benzyl group at N-1 position of the 1,4-benzodiazepin-2-one moiety (**11b**) was superior to the methyl, allyl, *iso*-butyl, methoxyethyl, and *N*-benzylacetamide groups at the corresponding position in terms of selectivities (**11h**, **11i**, **11j**, **11n**, and **11o**). The methyl group in **11k** and **11l** at C-5 position is slightly more favourable than the phenyl group (**11a** and **11f**) at the corresponding position as regards the selectivity. We observed that introduction of γ -turn mimicry^{10e} at the tail position resulted in almost no selectivity for Lck over c-Src (**11p** and **11q**).

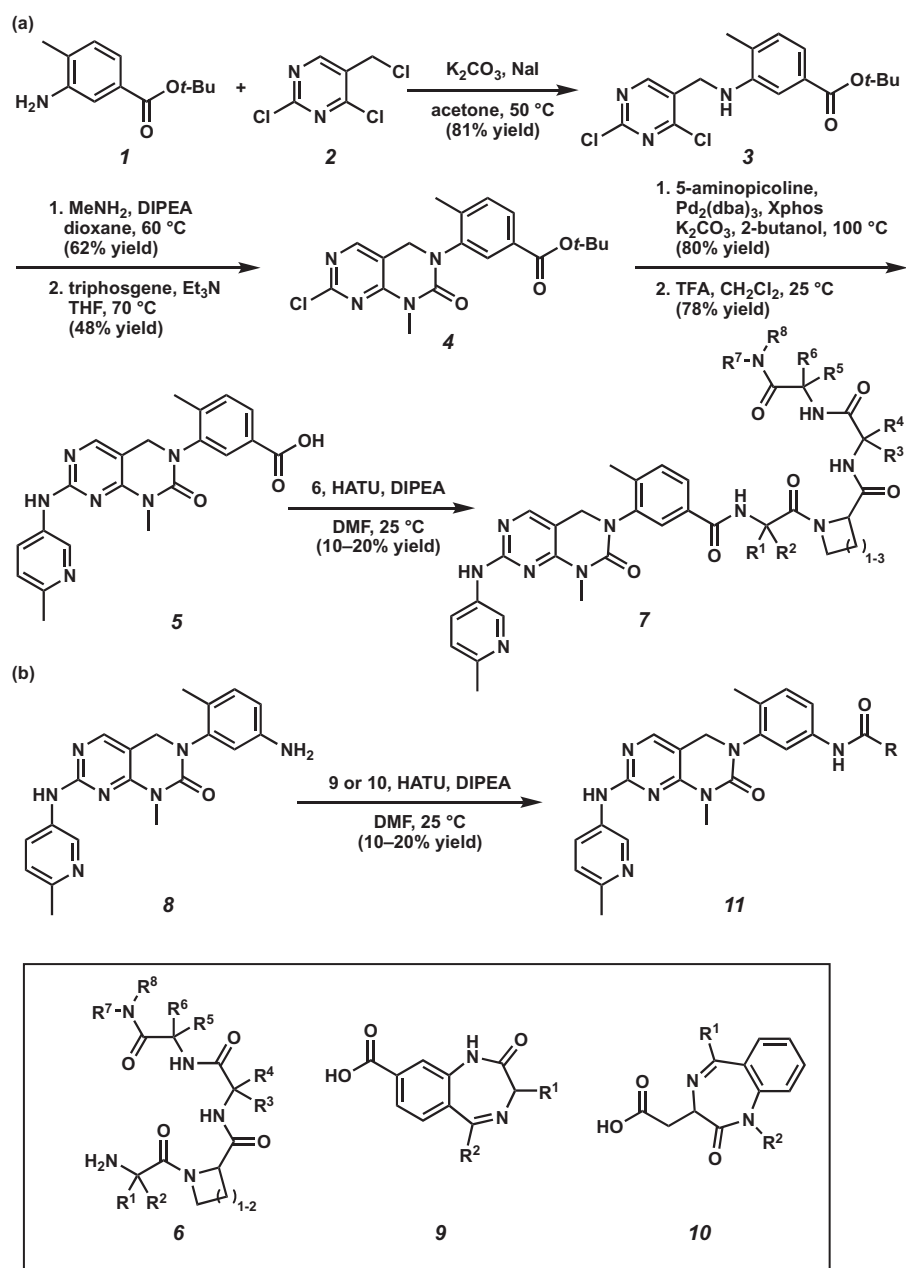
We explored *in vitro* potencies of **7a** and **11b** at both 14 μ M (Km) and 1 mM ATP concentrations to investigate whether these inhibitors are ATP competitive inhibitors (Table 4). We observed that the IC₅₀ values were increased dramatically at 1 mM ATP concentration compared to those at Km ATP concentrations. Thus, we concluded that both **7a** and **11b** are ATP competitive kinase inhibitors.

2.3. Kinome-wide selectivities of 7a described on a kinome phylogenetic tree

We were pleased to confirm that **7a** possesses higher selectivity for Lck over other 373 kinases at 1 μ M concentration compared to GNF 7 (Figure 2, Supplementary Table S1–S4). We also obtained IC₅₀ values of **7a** against five kinases (Lck, DDR1, Fgr, Bmx, and Blk), which were inhibited greater than 70% in the kinome-wide profiling analysis (Figure 2c, Supplementary Table S1). As shown in Figure 2(c), **7a** has an IC₅₀ value of 23 nM against Lck and possesses 5 to 13-fold selectivity over these four kinases. Furthermore, **7a** showed more than 10-fold selectivities over other structurally similar Src family kinases (Figure 2d).

2.4. Docking into Lck binding site

Docking of **7a** and **11b** with Lck kinase by long time (3 μ s) molecular dynamics (MD) simulation revealed that turn peptidomimetic scaffolds were located at an allosteric binding site. Also,



Scheme 1. (a) Synthesis of kinase inhibitors containing turn mimetic amide scaffolds. (b) Synthesis of kinase inhibitors possessing benzodiazepines.

hydrophobic groups of the peptidomimetic scaffolds interacted with the allosteric helix of the binding site (C-helix in Figure 3). The results reveal that the amide moiety of **7a** participates in hydrogen-bonding networks with Glu288 in Lck. Additionally, the phenyl group of **11b** interacts with Phe354 by π - π stacking interaction. The core scaffolds of **7a** and **11b** were interacted with kinases hinge region through similar binding poses of the crystal structure of imatinib with kinases (Supplementary Figure S1). The Asp from the "DFG-motif" interacts with the amide functional group of **7a** and **11b**. Moreover, phenyl moieties on the linker region of **7a** and **11b** interacts with Lys273 by cation- π interaction.

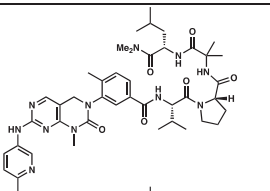
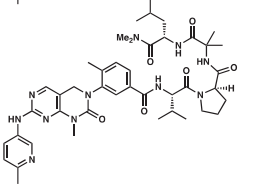
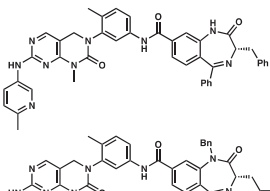
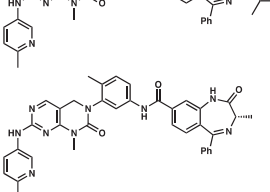
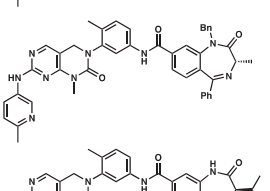
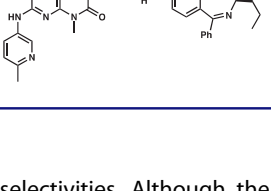
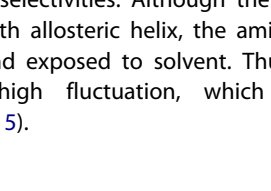
2.5. Watermap application

Next, we further analysed binding sites using WaterMap application^{11,12}. With WaterMap results, many hydration sites with

unstable energy ($0 > \text{kcal/mol}$) were found in the allosteric binding site (Supplementary Figure S2). Therefore, when **7a** was located at the unstable hydration sites, high binding free energy compensation could be obtained. Five hydration sites with a high energy of over 3.00 kcal/mol were found in Lck, and the peptidomimetic scaffold of **7a** occupied these sites (Figure 4). We envisioned that the energetically unstable regions at the allosteric site of Lck could be compensated with interaction of terminal turn peptidomimetic tail of **7a**, which would contribute to high selectivity of **7a** for Lck kinase.

With the interesting WaterMap calculation result, we attempted to explain the IC_{50} difference of **7a** and its enantiomer **7c** on Lck by the WaterMap application method (Figure 5). The U-shaped tail of **7a** is located in the allosteric binding site on Lck. Also, amino acids at i and $i+3$ of **7a** tail interact with allosteric helix. However, turn structure of **7c** is not fully located at the allosteric binding site of Lck, which is expected to be highly important for

Table 1. *In vitro* potency profiling on selected kinases.

compound	structure	Lck (IC ₅₀ , nM)	c-Src (IC ₅₀ , nM)	p38a (IC ₅₀ , nM)	Abi1 (IC ₅₀ , nM)
7a		23.0	861	>10000	378
7b		174	379	2050	317
11a		8.50	20.4	1830	189
11b		37.3	410	3430	453
11c		1.17	2.84	14.9	4.64
11d		3.42	15.2	101	24.1
11e		10.7	12.8	250	55.2

kinase selectivities. Although the amino acid at *i* of **7c** tail interacts with allosteric helix, the amino acid at *i* + 3 is extruded outside and exposed to solvent. Thus, the tail structure of **7c** could have high fluctuation, which results in lower selectivities (Figure 5).

2.6. Inhibitory effect of **7a** on Lck activation

We investigated whether Lck activation was affected by **7a** in Jurkat cell line (Figure 6). Western blot analysis revealed that **7a** markedly reduced the phosphorylated Lck levels at tyrosine 394 residue in a concentration-dependent manner in anti-CD3-treated Jurkat T cells. These results suggested that **7a** inhibited the anti-CD3-activated Lck, similar to positive control A770041.

2.7. In vivo experiment with dextran sulphate sodium (DSS)-induced colitis model

Inflammatory bowel disease (IBD), which is a chronic and immune-mediated disorder of the gastrointestinal tract encompasses Crohn's disease (CD) and ulcerative colitis (UC)¹³. Although the exact cause of IBD is unclear, it is widely accepted that an

excessive immune response against normal components of microflora results in IBD. Especially, excessive T cell activation plays a pivotal role in mucosal damage in both CD and UC¹⁴. Lck plays a crucial role in activation of TCR-linked signal transduction pathways, leading to T cell activation and proliferation¹⁵. Additionally, it is reported that overexpression of Lck leads to IBD¹⁵. Hence, we evaluated the potential of our selective Lck kinase inhibitor **7a** for IBD treatment with dextran sulphate sodium (DSS)-induced colitis model. DSS administration induces acute colonic damage, and changes in clinical parameters can be monitored¹⁶. To determine the recovery effect of **7a** in DSS-induced colitis, we assessed the clinical symptom including disease activity index (DAI) and colon length. The DAI scores were evaluated by body weight loss, stool consistency, and occult/gross bleeding (Table 5). During the administration of DSS (4%) for 7 days, DAI values were significantly increased (Figure 7a). We discovered that **7a** treatment (5 mg/kg, *i.p.*) improved the symptom changes at the end of experiments (Figure 7b). In addition, the colon length of DSS-treated group was significantly shorter than that of the vehicle-administered control group (8.17 ± 0.32 cm vs. 4.25 ± 0.38 cm, $p < 0.001$), while **7a** treatment (5 mg/kg, *i.p.*) recovered the DSS-induced colon shortening (4.25 ± 0.38 cm vs. 5.47 ± 0.60 cm, $p < 0.05$, Figure 7(C, D).

3. Conclusion

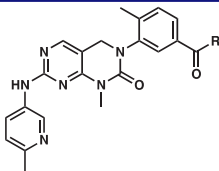
In conclusion, we discovered highly selective type II kinase inhibitors by introducing chiral turn peptidomimetic moieties on the tail region for the first time. It turned out that **7a**, a novel type II kinase inhibitor, is a potent and exceptionally selective Lck inhibitor. Based on kinome-wide selectivity profiling data, it was confirmed that **7a** possesses high selectivity. Kinases selectivities were highly affected by subtle changes of the substituents of peptidomimetic scaffolds. To the best of our knowledge, it has never been reported that low selectivity of a type II kinase inhibitor is dramatically enhanced by adopting chiral peptidomimetic tail. The western blot analysis revealed that **7a** is capable of inhibiting Lck activation in anti-CD3-treated Jurkat T cells. Finally, we discovered that **7a** could alleviate of clinical symptoms in DSS-induced colitis mice. This study may shed a bright light on the design of selective type II kinase inhibitors by adopting chiral peptidomimetic tails.

4. Experimental

4.1. Chemistry

4.1.1. General procedures

Unless otherwise stated, reactions were performed in flame-dried glassware under a nitrogen atmosphere using dry solvents. Reaction progress was monitored by thin-layer chromatography (TLC). Purified water was obtained using a Barnstead NANOpure Infinity UV/UF system. Brine solutions are saturated aqueous solutions of sodium chloride. Commercially available reagents were purchased from Sigma-Aldrich, Acros Organics, Combi-Blocks, TCI or Alfa Aesar and used as received unless otherwise stated. Reaction temperatures were controlled by an IKAmag temperature modulator unless otherwise indicated. TLC was performed using E. Merck silica gel 60 F254 precoated glass plates (0.25 mm) and visualised by UV fluorescence quenching, KMnO₄, or Ninhydrin staining. Silicycle SiliaFlash P60 Academic Silica gel (particle size 0.040–0.064 mm) was used for flash column chromatography. ¹H NMR spectra were recorded on Bruker 400 MHz and 600 MHz spectrometer and are reported relative to residual CDCl₃ (δ 7.26 ppm),

Table 2. *In vitro* potency profiling on Lck and c-Src.


compound	R	Lck (IC ₅₀ , nM)	c-Src (IC ₅₀ , nM)	selectivity index (Lck IC ₅₀ /c-Src IC ₅₀)	compound	R	Lck (IC ₅₀ , nM)	c-Src (IC ₅₀ , nM)	selectivity index (Lck IC ₅₀ /c-Src IC ₅₀)
7a		23.0	861	37	7m		379	3970	10
7c		211	735	3.5	7n		727	3140	4.3
7d		49.0	555	11	7o		1040	> 10000	>9.6
7e		129	2080	16	7p		55.6	329	5.9
7f		27.5	658	24	7q		15.4	174	11
7g		40.2	1370	34	7r		216	577	2.7
7h		64.4	1740	27	7s		36.0	435	12
7i		61.5	123	2.0	7t		70.8	477	6.7
7j		18.0	586	33	7u		174	1140	6.6
7k		302	921	3.0	7v		403	5630	14
7l		155	1740	11	7w		129	585	4.5

CD₃OD (δ 3.31 ppm) or (CD₃)₂SO (δ 2.50 ppm). ¹³C NMR spectra are recorded on Bruker 400 MHz and 600 MHz spectrometer (101 MHz & 151 MHz) and are reported relative to CDCl₃ (δ 7.26 ppm), CD₃OD (δ 3.31 ppm) or (CD₃)₂SO (δ 2.50 ppm). ¹⁹F NMR

spectrum is recorded on Bruker 600 MHz spectrometer (377 MHz) and is reported relative to (CD₃)₂SO (δ 2.50 ppm). Data for ¹H NMR are reported as follows: s=singlet, d=doublet, t=triplet, q=quartette, p=pentet, sept=septuplet, m=multiplet, br

Table 3. *In vitro* potency profiling on Lck and c-Src.

compound	R	Lck (IC ₅₀ , nM)	c-Src (IC ₅₀ , nM)	selectivity index (Lck IC ₅₀ /Src IC ₅₀)	compound	R	Lck (IC ₅₀ , nM)	c-Src (IC ₅₀ , nM)	selectivity index (Lck IC ₅₀ /Src IC ₅₀)
11b		37.3	410	11	11l		4.63	19.6	4.2
11f		18.7	62.6	3.3	11m		1.05	4.01	3.8
11g		42.1	134	3.2	11n		16.0	48.6	3.0
11h		24.6	135	5.5	11o		27.8	87.5	3.1
11i		49.3	222	4.5	11p		3.80	6.14	1.6
11j		132	461	3.5	11q		17.9	24.8	1.4
11k		3.57	27.1	7.6					

Table 4. Biochemical IC₅₀ values of **7a** and **11b** on Lck at Km and 1 mM ATP concentration.

Kinase	ATP conc.	IC ₅₀ (nM)		
		7a	11b	Staurosporine (ref)
Lck	14 μM	190	510	1.32
Lck	1 mM	21000	>100000	15.6

s = broad singlet, br d = broad doublet, app = apparent. Data for ¹³C are reported in terms of chemical shifts (δ ppm). Data for ¹⁹F is reported in terms of chemical shifts (δ ppm). The purity of final compounds was determined to be ≥95% using HPLC analyses performed on an Agilent 1100 series with a Poroshell C18 column (pore size: 120 Å; particle size: 4 μm, dimensions: 4.6 × 150 mm). Some final compounds are purified using PREP HPLC performed on an Agilent 1260 Infinity II with Agilent Prep-C18 column (particle size: 10 μm, dimensions: 250 × 21.2 mm). IR spectra were obtained using a Nicolet Avatar 330 FT-IR spectrometer and Bruker Alpha Platinum-ATR using thin films deposited on NaCl plates and reported in frequency of absorption (cm⁻¹). Optical rotations were measured with a Rudolph AUTOPOL I automatic polarimeter

operating on the sodium D-line (589 nm), using a 100 nm path-length cell and are reported as: [α]_D^T (concentration in g/100 ml, solvent). High resolution mass spectra (HRMS) were obtained from Waters SYNAPT G2 TOF with a Waters Multimode source in electrospray ionisation (ESI+), atmospheric pressure chemical ionisation (APCI+), or mixed ionisation mode (MM: ESI-APCI+).

4.1.2. *Tert*-butyl 3-amino-4-methylbenzoate (**1**)

To a solution of *tert*-butyl 4-methyl-3-nitrobenzoate (113 mg, 0.475 mmol, 1.00 equiv) in EtOH (1.18 ml) was added Pd/C (24.0 mg, 0.574 mmol), cyclohexene (1.18 ml). The reaction mixture was stirred for 16 h at 80 °C. Solids were removed via a filtration through a celite plug and the resulting solution was concentrated under reduced pressure. The filtrate was purified by flash column chromatography (4:1 hexanes:EtOAc) on silica gel to give aminobenzoate **1** (91.0 mg, 92% yield) as a yellow liquid. *R*_f: 0.55 (4:1 hexanes:EtOAc); ¹H NMR (400 MHz, DMSO) δ 7.17 (d, *J* = 1.4 Hz, 1H), 7.00 (t, *J* = 1.2 Hz, 2H), 5.07 (s, 2H), 2.08 (s, 3H), 1.51 (s, 9H); ¹³C NMR (101 MHz, DMSO) δ 165.60, 146.64, 129.79, 129.70, 126.17, 116.80, 114.09, 79.75, 30.69, 27.87, 17.57; IR (Neat) 3470,

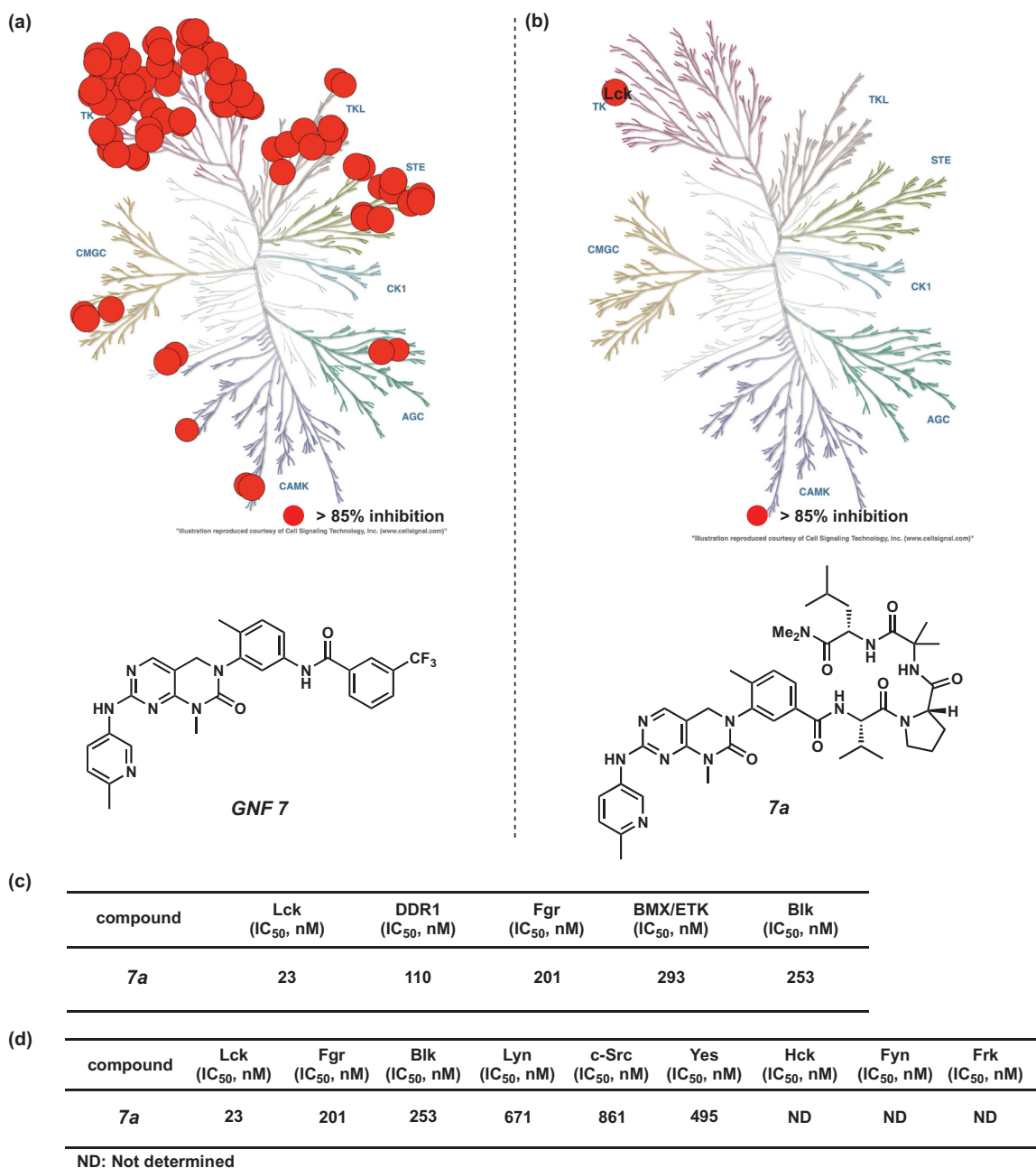


Figure 2. This illustration was reproduced courtesy of Cell Signalling Technology, Inc. (www.cellsignal.com). (a) Kinome phylogenetic tree description of the GNF 7 selectivity profile. (b) Kinome-wide selectivities of 7a described on a kinome phylogenetic tree. (c) *In vitro* IC₅₀ values of 7a against kinases, which were inhibited greater than 70%. (d) *In vitro* IC₅₀ values of 7a against Src family kinases.

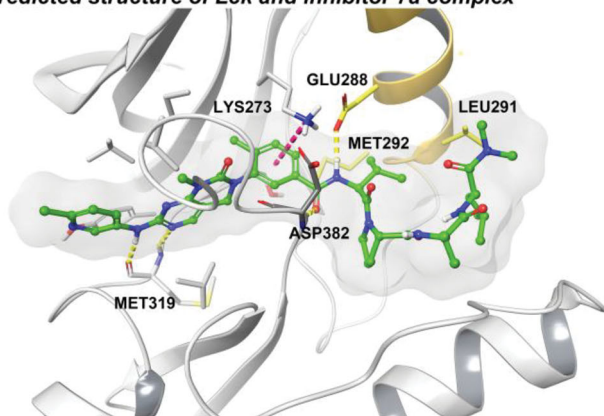
3377, 2975, 2927, 2857, 1697, 1625, 1577, 1508, 1477, 1456, 1423, 1392, 1367, 1300, 1247, 1164, 1144, 1108, 1071, 1032, 997, 948, 886, 851, 825, 760, 642, 562, 527, 440 cm⁻¹; HRMS (MM: ESI-APCI+) m/z calc'd for C₁₂H₁₈NO₂ [M+H]⁺: 208.1338; found: 208.1334.

4.1.3. *Tert-butyl 3-(((2,4-dichloropyrimidin-5-yl)methyl)amino)-4-methylbenzoate (3)*

To a solution of aminobenzoate **1** (1.20 g, 5.97 mmol, 1.00 equiv), 2,4-dichloro-5-(chloromethyl)pyrimidine **2** (1.40 g, 7.16 mmol, 1.20 equiv) in acetone (7.46 ml) was added NaI (1.34 g, 8.95 mmol, 1.50 equiv), K₂CO₃ (1.34 g, 11.3 mmol, 1.90 equiv). The reaction mixture was stirred for 10 h at 50 °C. The resulting suspension

was filtered and washed with CH₂Cl₂. The filtrate was concentrated *in vacuo* and purified by flash column chromatography (4:1 hexanes:EtOAc) on silica gel to give dichloropyrimidine **3** (2.10 g, 81% yield) as an orange liquid. *R*_f: 0.5 (4:1 hexanes:EtOAc); ¹H NMR (400 MHz, CDCl₃) δ 8.51 (s, 1H), 7.36 (dd, *J* = 7.7, 1.6 Hz, 1H), 7.13 (dd, *J* = 7.7, 0.8 Hz, 1H), 7.07 (d, *J* = 1.6 Hz, 1H), 4.55 (s, 2H), 2.25 (s, 3H), 1.55 (s, 9H); ¹³C NMR (101 MHz, CDCl₃) δ 165.97, 161.40, 159.49, 159.38, 144.22, 131.17, 130.41, 129.61, 127.51, 119.87, 110.29, 80.90, 42.65, 28.23, 17.72; IR (Neat) 3411, 2977, 2931, 1699, 1610, 1580, 1560, 1519, 1474, 1450, 1422, 1384, 1367, 1349, 1299, 1247, 1163, 1115, 1093, 1065, 1032, 993, 951, 916, 856, 819, 798, 760, 732, 703, 687, 648, 468, 439, 419 cm⁻¹; HRMS (MM: ESI-APCI+) m/z calc'd for C₁₇H₁₉Cl₂N₃O₂Na [M+Na]⁺: 390.0754; found: 390.0745.

(a) predicted structure of Lck and inhibitor 7a complex



(b) predicted structure of Lck and inhibitor 11b complex

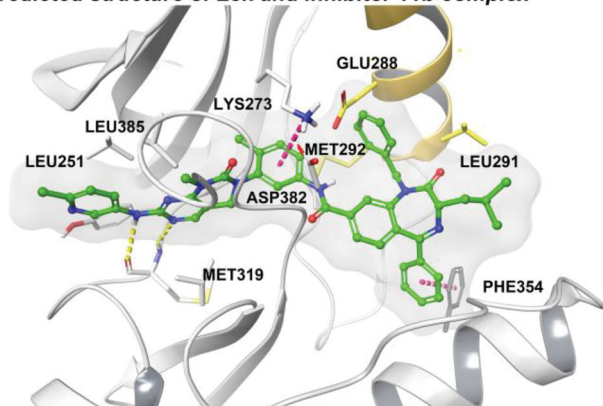


Figure 3. (a) Predicted structure of Lck and 7a complex. (b) Predicted structure of Lck and 11b complex. (red dashed line: π - π interaction/cation- π interaction, yellow dashed line: hydrogen-bonding).

4.1.4. *Tert*-butyl 3-(7-chloro-1-methyl-2-oxo-1,4-dihydropyrimido[4,5-d]pyrimidin-3(2H)-yl)-4-methylbenzoate (4)

To a solution of dichloropyrimidine **3** (1.50 g, 4.00 mmol, 1.00 equiv) in 1,4-dioxane (13.6 ml) was added MeNH_2 (8.14 ml, 8.14 mmol, 1.50 equiv), *i*-Pr₂NEt (2.12 ml, 12.2 mmol, 3.00 equiv). The reaction mixture was stirred for 1.5 h at 60 °C and then diluted with CH_2Cl_2 and water. The aqueous phase was extracted with CH_2Cl_2 . The combined organic phases were washed with brine, dried over MgSO_4 and concentrated *in vacuo*. The residue was purified by flash column chromatography (1:1 hexane:EtOAc) on silica gel to give *tert*-butyl 3-(((2-chloro-4-(methylamino)pyrimidin-5-yl)methyl)amino)-4-methylbenzoate (0.920 g, 62% yield) as a pale-yellow liquid. R_f : 0.18 (4:1 hexanes:EtOAc); $^1\text{H NMR}$ (400 MHz, CDCl_3) δ 7.94 (s, 1H), 7.45 (dd, $J=7.7, 1.6$ Hz, 1H), 7.39 (d, $J=1.6$ Hz, 1H), 7.15 (d, $J=7.8$ Hz, 1H), 4.20 (s, 2H), 3.04 (d, $J=4.9$ Hz, 3H), 2.19 (s, 3H), 1.59 (s, 9H); $^{13}\text{C NMR}$ (101 MHz, CDCl_3) δ 166.08, 163.32, 160.61, 154.74, 145.11, 131.32, 130.36, 128.86, 120.96, 112.60, 112.05, 81.11, 43.76, 28.36, 28.11, 17.92; IR (Neat) 3361, 2955, 2923, 2853, 1705, 1597, 1580, 1514, 1455, 1423, 1397, 1367, 1342, 1300, 1270, 1247, 1166, 1115, 1069, 1031, 992, 934, 873, 851, 779, 761, 737, 700, 517, 463 cm^{-1} ; HRMS (MM: ESI-APCI+) m/z calc'd for $\text{C}_{18}\text{H}_{24}\text{ClN}_4\text{O}_2$ $[\text{M} + \text{H}]^+$: 363.1588; found: 363.1585.

To a solution of *tert*-butyl 3-(((2-chloro-4-(methylamino)pyrimidin-5-yl)methyl)amino)-4-methylbenzoate (0.500 g, 1.40 mmol, 1.00 equiv) in THF (4.60 ml) was added triphosgene (0.200 g, 0.700 mmol, 0.500 equiv), Et_3N (0.950 ml, 7.00 mmol, 5.00 equiv) at 0 °C under N_2 atmosphere. The reaction mixture was stirred for

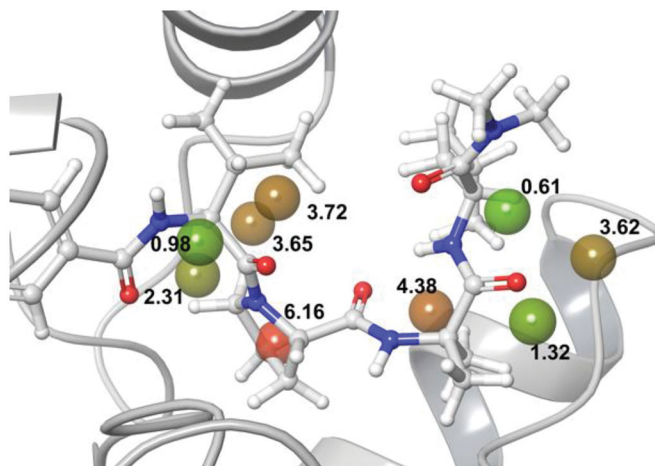


Figure 4. Analysis results of Lck and superimpose of 7a at the allosteric site by using WaterMap application. Coloured sphere: hydration sites occupied by the inhibitor. The number on the sphere: ΔG energy (kcal/mol). Green sphere: low energy. Red sphere: high energy over 5 kcal/mol.

1 h at 70 °C and then diluted with CH_2Cl_2 and water. The aqueous phase was extracted with CH_2Cl_2 . The combined organic phases were washed with brine, dried over MgSO_4 and concentrated *in vacuo* and washed with isopropyl ether to give methyl urea **4** (0.920 g, 62% yield) as a pale-yellow solid. R_f : 0.66 (1:1 hexane:EtOAc); $^1\text{H NMR}$ (400 MHz, CDCl_3) δ 8.12 (s, 1H), 7.90 (dd, $J=7.9, 1.7$ Hz, 1H), 7.84 (d, $J=1.7$ Hz, 1H), 7.36 (d, $J=8.0$ Hz, 1H), 4.83 (d, $J=14.8$ Hz, 1H), 4.55 (d, $J=14.8$ Hz, 1H), 3.47 (s, 3H), 2.28 (s, 3H), 1.58 (s, 9H); $^{13}\text{C NMR}$ (101 MHz, CDCl_3) δ 164.89, 160.45, 158.98, 153.47, 151.88, 140.88, 140.32, 131.86, 131.48, 129.55, 128.06, 110.34, 81.54, 47.15, 29.05, 28.33, 18.01; IR (Neat) 2978, 1688, 1584, 1471, 1432, 1395, 1360, 1336, 1288, 1253, 1212, 1157, 1143, 1126, 1107, 1069, 1035, 976, 932, 874, 849, 825, 791, 764, 749, 734, 694, 637, 531, 475, 454, 418 cm^{-1} ; HRMS (MM: ESI-APCI+) m/z calc'd for $\text{C}_{19}\text{H}_{22}\text{ClN}_4\text{O}_3$ $[\text{M} + \text{H}]^+$: 389.1380; found: 389.1378.

4.1.5. 4-Methyl-3-(1-methyl-7-((6-methylpyridin-3-yl)amino)-2-oxo-1,4-dihydropyrimido[4,5-d]pyrimidin-3(2H)-yl)benzoic acid (5)

To a solution of methyl urea **4** (1.70 g, 4.50 mmol, 1.00 equiv) in butan-2-ol (22.5 ml) was added 5-aminopycoline (0.500 g, 4.54 mmol, 1.01 equiv), K_2CO_3 (3.10 g, 22.5 mmol, 5.00 equiv), Xphos (0.400 g, 0.800 mmol, 0.200 equiv), $\text{Pd}_2(\text{dba})_3$ (0.800 g, 0.800 mmol, 0.200 equiv). The reaction mixture was stirred for 2 h at 100 °C. Solids were removed via a filtration through a celite plug and the resulting solution was concentrated under reduced pressure. The filtrate was purified by flash column chromatography (1:20 to 1:10 MeOH: CH_2Cl_2) on silica gel to give *tert*-butyl 4-methyl-3-(1-methyl-7-((6-methylpyridin-3-yl)amino)-2-oxo-1,4-dihydropyrimido[4,5-d]pyrimidin-3(2H)-yl)benzoate (1.65 g, 80% yield) as a white solid. R_f : 0.53 (1:1 hexane:THF); $^1\text{H NMR}$ (400 MHz, CDCl_3) δ 8.74 (d, $J=2.6$ Hz, 1H), 8.01 (dd, $J=8.4, 2.7$ Hz, 1H), 7.99 (s, 1H), 7.88 (dd, $J=7.9, 1.8$ Hz, 1H), 7.85 (d, $J=1.7$ Hz, 1H), 7.34 (d, $J=7.9$ Hz, 1H), 7.29 (s, 1H), 7.16 (d, $J=8.4$ Hz, 1H), 4.75 (dd, $J=13.8, 1.1$ Hz, 1H), 4.52–4.41 (m, 1H), 3.45 (s, 3H), 2.56 (s, 3H), 2.28 (s, 3H), 1.58 (s, 9H); $^{13}\text{C NMR}$ (101 MHz, CDCl_3) δ 164.89, 159.20, 157.76, 152.73, 152.61, 151.96, 140.87, 140.73, 140.03, 133.83, 131.51, 131.17, 129.10, 128.02, 127.45, 123.15, 103.08, 81.25, 47.38, 28.72, 28.19, 23.43, 17.90; IR (Neat) 3277, 2956, 2925, 2854, 1709, 1681, 1605, 1576, 1532, 1491, 1413, 1369, 1331, 1290, 1255, 1235, 1167, 1126, 1071, 1032, 951, 848, 786, 752, 682, 643,

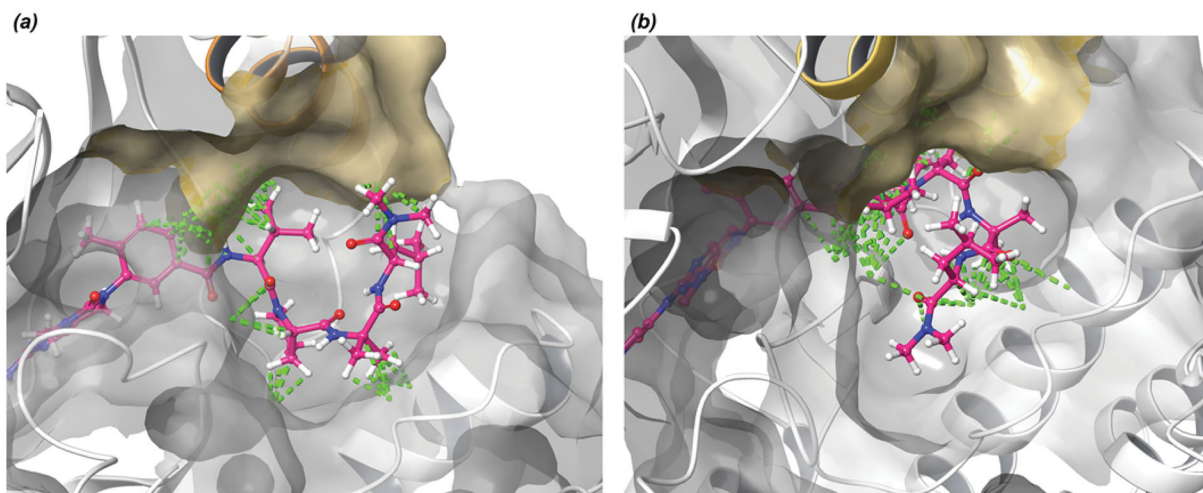


Figure 5. (a) Analysis results of Lck and superimpose of turn scaffold of **7a** at the allosteric site by using WaterMap application. (b) Analysis results of Lck and superimpose of turn scaffold of **7c**, which is enantiomer of **7a** at the allosteric site by using WaterMap application. (green dashed line: van der Waals interaction).

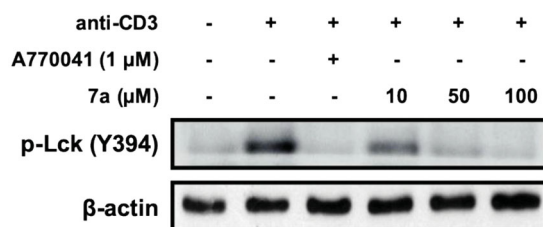


Figure 6. Effect of **7a** on the Lck (Y394) activation in anti-CD3-treated Jurkat cells. After treatment with CD3 antibody for coating in plates, cells were seeded and then treated with various concentrations of **7a** (10, 50, or 100 μ M) or A770041 (1 μ M) used as a positive control. The phosphorylation of Lck tyrosine in Jurkat cells was activated by anti-CD3 mAb. Total cellular protein was resolved by SDS-PAGE, transferred to PVDF membranes, and detected with specific p-Lck (Y394) antibody. β -Actin was used as an internal control.

520, 454 cm^{-1} ; HRMS (MM: ESI-APCI+) m/z calc'd for $\text{C}_{25}\text{H}_{29}\text{N}_6\text{O}_3$ $[\text{M} + \text{H}]^+$: 461.2301; found: 461.2301.

To a solution of *tert*-butyl 4-methyl-3-(1-methyl-7-((6-methylpyridin-3-yl)amino)-2-oxo-1,4-dihydropyrimido[4,5-d]pyrimidin-3(2*H*)-yl)benzoate (0.460 g, 1.00 mmol, 1.00 equiv) in CH_2Cl_2 (10.0 ml) was added trifluoroacetic acid (1.50 ml, 20.0 mmol, 20.0 equiv). The reaction mixture was stirred for 12 h at 23 $^\circ\text{C}$. The resulting solution was concentrated under reduced pressure and washed with ether to give benzoic acid **5** (0.400 g, 78% yield) as a white solid. R_f : 0.13 (1:10 MeOH: CH_2Cl_2); ^1H NMR (400 MHz, MeOD) δ 9.49 (d, J = 2.5 Hz, 1H), 8.47 (dd, J = 8.9, 2.6 Hz, 1H), 8.22 (d, J = 1.1 Hz, 1H), 7.98 (d, J = 1.8 Hz, 1H), 7.94 (dd, J = 7.9, 1.8 Hz, 1H), 7.80 (d, J = 8.9 Hz, 1H), 7.45 (d, J = 8.0 Hz, 1H), 4.83 (d, J = 1.1 Hz, 1H), 4.61 (dd, J = 14.2, 0.9 Hz, 1H), 3.47 (s, 3H), 2.72 (s, 3H), 2.30 (s, 3H); ^{13}C NMR (101 MHz, MeOD) δ 167.51, 158.20, 157.69, 153.21, 152.77, 145.38, 141.51, 140.91, 138.76, 134.47, 131.06, 130.09, 129.12, 129.05, 128.40, 127.49, 105.25, 46.79, 27.77, 17.36, 16.47. IR (Neat) 3041, 2923, 1674, 1602, 1566, 1503, 1467, 1421, 1340, 1286, 1265, 1234, 1182, 1128, 1107, 1068, 1024, 872, 840, 795, 767, 745, 720, 704, 683, 640, 618, 564, 517, 447 cm^{-1} ; HRMS (MM: ESI-APCI+) m/z calc'd for $\text{C}_{21}\text{H}_{21}\text{N}_6\text{O}_3$ $[\text{M} + \text{H}]^+$: 405.1675; found: 405.1674.

4.1.6. General Procedure a for synthesis of amides **7**

To a solution of benzoic acid **5** (1.20 equiv) in DMF (0.100 M) was added amine **6** (1.00 equiv), *i*-Pr₂NEt (5.00 equiv), HATU (2.00 equiv). The reaction mixture was stirred for 12 h at 23 $^\circ\text{C}$ and then diluted with CH_2Cl_2 and sat. NaHCO_3 . The aqueous phase was

extracted with CH_2Cl_2 . The combined organic phases were washed with brine, dried over MgSO_4 and concentrated *in vacuo*. The residue was purified by flash column chromatography (1:10 MeOH: CH_2Cl_2) on silica gel to give amide **7** (10–20% yield) as a white solid.

4.1.7. General Procedure B for synthesis of amides **11**

To a solution of aniline **8** (1.20 equiv) and carboxylic acid **9** or **10** (1.00 equiv) in DMF (0.100 M) was added HATU (2.00 equiv) and *i*-Pr₂NEt (5.00 equiv) at 23 $^\circ\text{C}$. The reaction mixture was stirred for 16 h at 23 $^\circ\text{C}$. The reaction was diluted with CH_2Cl_2 and quenched by addition of sat. NaHCO_3 . The phases were separated and the aqueous phase was extracted with EtOAc. The combined organic layer was washed with brine, dried over MgSO_4 , and concentrated *in vacuo*. The residue was purified by column chromatography (1:20 MeOH: CH_2Cl_2) on silica gel to afford amide **11** (10–20% yield).

Note: Spectra of compounds **7** were also acquired in methanol-*d* or acetone-*d*. The integrations of the major and minor peaks changed, providing evidence that species are indeed conformers/rotamers.

4.1.8. (*S*)-*N*-(1-(((*S*)-1-(dimethylamino)-4-methyl-1-oxopentan-2-yl)amino)-2-methyl-1-oxopropan-2-yl)-1-(((4-methyl-3-(1-methyl-7-((6-methylpyridin-3-yl)amino)-2-oxo-1,4-dihydropyrimido[4,5-d]pyrimidin-3(2*H*)-yl)benzoyl)-*L*-valyl)pyrrolidine-2-carboxamide (**7a**)

(Due to the distinct presence of rotameric isomers, the ^1H NMR and ^{13}C NMR contained extra peaks. See the attached spectrum in the supporting information) (Purity: 99%; HPLC); R_f : 0.35 (1:10 = MeOH: CH_2Cl_2); $[\alpha]_{\text{D}}^{28} = -102$ (c 0.0590, MeOH); ^1H NMR (400 MHz, DMSO) δ 9.64 (s, 1H), 8.79 (d, J = 2.7 Hz, 1H), 8.42 (d, J = 8.0 Hz, 1H), 8.14 (s, 1H), 8.05 (dd, J = 8.5, 2.7 Hz, 1H), 8.00 (s, 1H), 7.93 (dd, J = 22.4, 1.8 Hz, 1H), 7.87–7.77 (m, 1H), 7.40 (d, J = 8.0 Hz, 1H), 7.27 (d, J = 8.5 Hz, 1H), 7.17 (d, J = 8.5 Hz, 1H), 4.86–4.66 (m, 2H), 4.56–4.44 (m, 2H), 4.28 (dd, J = 7.8, 4.8 Hz, 1H), 3.89 (d, J = 9.6 Hz, 1H), 3.63 (t, J = 8.2 Hz, 1H), 3.32 (s, 3H), 2.98 (s, 3H), 2.78 (s, 3H), 2.40 (s, 3H), 2.20 (s, 3H), 2.15 (d, J = 23.1 Hz, 1H), 2.07–1.91 (m, 2H), 1.86 (q, J = 5.6 Hz, 2H), 1.50 (dq, J = 11.4, 5.7, 5.1 Hz, 1H), 1.46–1.40 (m, 1H), 1.40–1.37 (m, 1H), 1.35 (s, 3H), 1.30 (s, 3H), 1.02–0.92 (m, 6H), 0.85 (dd, J = 11.2, 6.3 Hz, 6H); ^{13}C NMR (101 MHz, DMSO) δ 173.25, 171.11, 170.96,

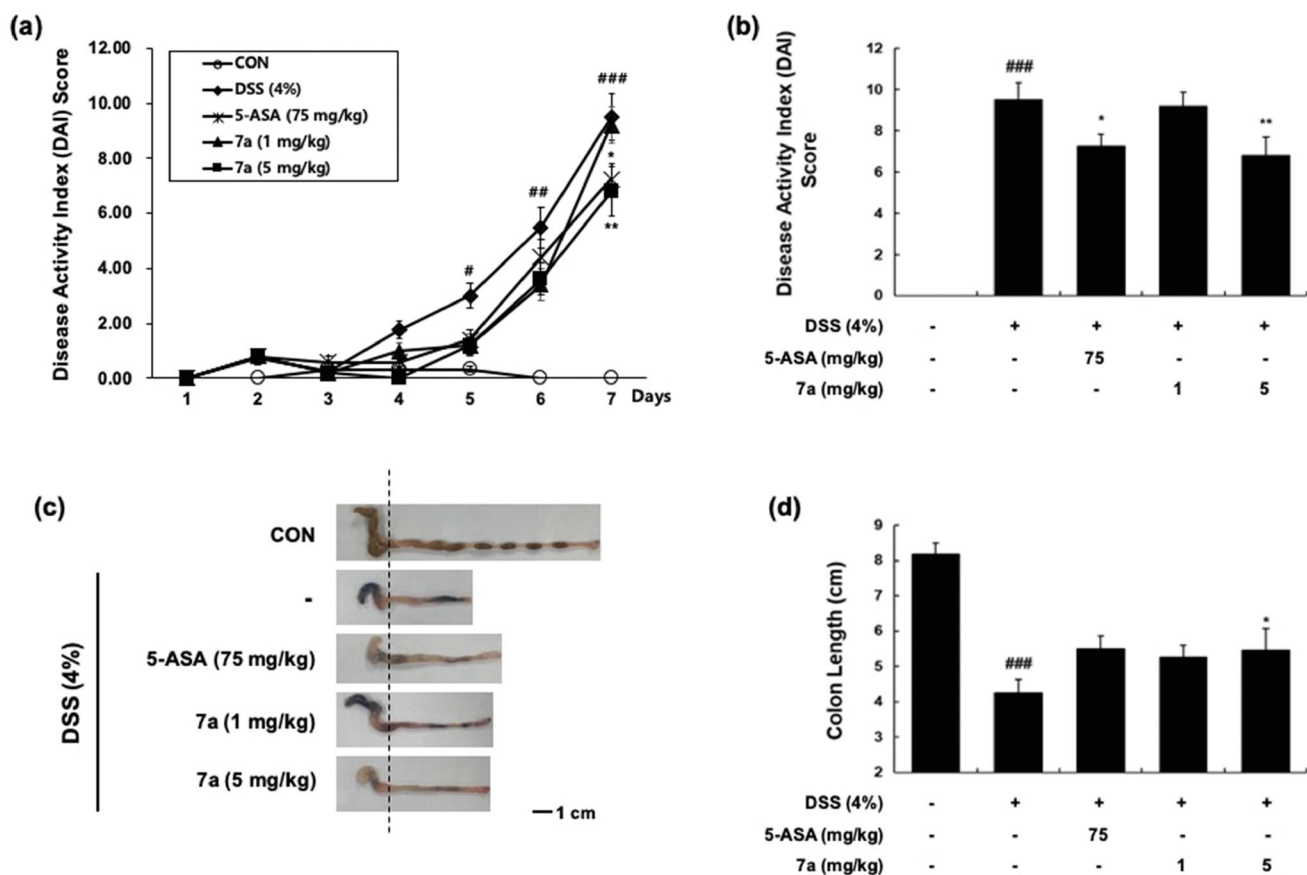


Figure 7. Effect of 7a on the progression of DSS-induced colitis. (a) Disease activity index (DAI) levels during total experiments periods and (b) at the end of the experiment (day 7). (c, d) Colon length was measured at the end of the experiment (day 7). Data are presented as mean \pm SE ($n=6$). # $p < 0.05$, ## $p < 0.01$, ### $p < 0.001$ vs. the vehicle-treated control group; * $p < 0.05$, ** $p < 0.01$ vs. the DSS-treated group. The significance between groups was determined by ANOVA and Dunnett's post-hoc test.

Table 5. Assessment of the disease activity index (DAI)

DAI score	Bodyweight loss (%)	Stool consistency	Occult/gross bleeding
0	None	Normal	Negative
1	1–5		
2	5–10	Loose stools	Hemoccult positive
3	10–20		
4	>20	Diarrhea	Gross bleeding

170.19, 170.14, 165.56, 165.39, 158.93, 156.93, 153.29, 153.22, 152.17, 152.12, 150.23, 141.10, 141.05, 140.04, 139.26, 134.68, 132.84, 132.74, 130.62, 126.84, 126.78, 126.56, 126.50, 126.24, 122.46, 102.91, 59.92, 59.88, 56.76, 55.99, 47.32, 46.69, 46.57, 40.91, 36.41, 35.13, 29.87, 28.88, 28.21, 25.41, 25.38, 24.70, 24.68, 24.59, 24.07, 23.23, 22.99, 22.97, 21.94, 21.92, 19.14, 19.06, 19.01, 17.28, 17.26; IR (Neat) 3300, 2959, 1632, 1607, 1530, 1496, 1411, 1332, 1240, 1174, 733 cm^{-1} ; HRMS (MM: ESI-APCI+) m/z calc'd for $\text{C}_{43}\text{H}_{60}\text{N}_{11}\text{O}_6$ $[\text{M} + \text{H}]^+$: 826.4728; found: 826.4734.

4.1.9. (R)-N-(1-((S)-1-(dimethylamino)-4-methyl-1-oxopentan-2-yl)amino)-2-methyl-1-oxopropan-2-yl)-1-((4-methyl-3-(1-methyl-7-((6-methylpyridin-3-yl)amino)-2-oxo-1,4-dihydropyrimido[4,5-d]pyrimidin-3(2H)-yl)benzoyl)-L-valyl)pyrrolidine-2-carboxamide (7b)

(Due to the distinct presence of rotameric isomers, the ^1H NMR and ^{13}C NMR contained extra peaks. See the attached spectrum in the supporting information) (Purity: 96%; HPLC); R_f : 0.34 (1:10 = MeOH:CH₂Cl₂); $[\alpha]_D^{30} = -176.0$ (c 0.00063, MeOH); ^1H NMR (400 MHz, DMSO) δ 9.64 (d, $J=7.0$ Hz, 2H), 8.79 (t, $J=2.2$ Hz, 2H),

8.71 – 8.46 (m, 2H), 8.18 – 8.11 (m, 2H), 8.05 (dd, $J=8.5$, 2.7 Hz, 2H), 8.00 – 7.87 (m, 3H), 7.86 – 7.70 (m, 3H), 7.41 (dt, $J=21.0$, 8.1 Hz, 4H), 7.18 (d, $J=8.5$ Hz, 2H), 4.84 – 4.59 (m, 4H), 4.56 – 4.36 (m, 4H), 4.30 (d, $J=10.6$ Hz, 2H), 3.85 – 3.52 (m, 5H), 3.05 – 2.79 (m, 6H), 2.66 (d, $J=23.7$ Hz, 6H), 2.40 (s, 6H), 2.21 – 2.16 (m, 6H), 2.06 – 1.93 (m, 3H), 1.87 (s, 3H), 1.61 (t, $J=8.8$ Hz, 3H), 1.39 (d, $J=34.3$ Hz, 3H), 1.32 (d, $J=5.0$ Hz, 2H), 1.28 (d, $J=5.6$ Hz, 6H), 1.23 (s, 6H), 1.03 (d, $J=6.1$ Hz, 7H), 0.95 (t, $J=6.7$ Hz, 9H), 0.90 – 0.86 (m, 3H), 0.84 (dt, $J=7.7$, 3.8 Hz, 12H); ^{13}C NMR (151 MHz, DMSO) δ 173.91, 173.79, 173.78, 173.76, 173.53, 173.50, 171.99, 171.95, 171.93, 171.82, 171.62, 171.60, 171.37, 170.53, 166.74, 159.71, 159.65, 159.29, 157.28, 157.24, 152.78, 152.49, 150.91, 150.56, 141.41, 140.38, 139.70, 135.05, 134.96, 133.53, 130.78, 126.58, 123.11, 122.83, 103.26, 60.39, 57.43, 56.37, 47.65, 47.62, 47.28, 47.13, 47.11, 47.08, 46.92, 46.79, 36.90, 35.53, 29.90, 28.90, 28.58, 26.68, 26.45, 26.23, 25.97, 25.34, 25.09, 24.79, 24.73, 24.32, 24.09, 23.75, 23.60, 23.58, 23.54, 23.52, 22.04, 21.85, 21.79, 21.73, 19.84, 19.53, 19.49, 19.27, 19.22, 17.71, 17.34; IR (Neat) 3306, 2922, 2852, 1720, 1670, 1631, 1600, 1572, 1531, 1404, 1333, 1294, 1259, 1152, 1025, 1006, 817, 756, 732, 699, 668 cm^{-1} ; HRMS (MM: ESI-APCI+) m/z calc'd for $\text{C}_{43}\text{H}_{60}\text{N}_{11}\text{O}_6$ $[\text{M} + \text{H}]^+$: 826.4728; found: 826.4738.

4.1.10. (S)-3-benzyl-N-(4-methyl-3-(1-methyl-7-((6-methylpyridin-3-yl)amino)-2-oxo-1,4-dihydropyrimido[4,5-d]pyrimidin-3(2H)-yl)phenyl)-2-oxo-5-phenyl-2,3-dihydro-1H-benzo[e][1,4]diazepine-8-carboxamide (11a)

(Purity: 96%; HPLC); R_f : 0.35 (1:10 MeOH:CH₂Cl₂); $[\alpha]_D^{25} = +90.7$ (c 0.150, MeOH); ^1H NMR (400 MHz, DMSO) δ 10.83 (s, 1H), 10.50 (s,

1H), 9.64 (s, 1H), 8.80 (d, $J=2.6$ Hz, 1H), 8.16 (d, $J=1.6$ Hz, 1H), 8.05 (dd, $J=8.4, 2.6$ Hz, 1H), 7.83 (dd, $J=4.0, 2.1$ Hz, 1H), 7.76 (s, 1H), 7.69 (dd, $J=8.2, 1.7$ Hz, 1H), 7.59 (dd, $J=8.4, 2.2$ Hz, 1H), 7.51 (dt, $J=8.6, 4.2$ Hz, 1H), 7.44 (d, $J=4.4$ Hz, 4H), 7.40–7.24 (m, 6H), 7.18 (dd, $J=8.0, 5.8$ Hz, 2H), 4.71 (d, $J=14.0$ Hz, 1H), 4.52 (d, $J=14.0$ Hz, 1H), 3.73 (dd, $J=8.1, 5.5$ Hz, 1H), 3.42 (td, $J=18.2, 16.0, 6.9$ Hz, 2H), 3.32 (s, 3H), 2.40 (s, 3H), 2.13 (s, 3H); ^{13}C NMR (101 MHz, DMSO) δ 170.58, 167.78, 164.89, 159.42, 157.49, 153.73, 152.56, 150.69, 141.65, 140.51, 139.76, 139.67, 139.01, 138.21, 135.18, 131.35, 131.25, 131.20, 130.93, 130.19, 129.78, 129.14, 128.81, 128.55, 126.71, 126.51, 122.93, 121.84, 121.21, 120.08, 119.52, 119.49, 103.42, 65.58, 47.12, 37.61, 28.71, 23.71, 17.28; IR (Neat) 3357, 2923, 2853, 1667, 1461, 1376, 1256, 1079, 746, 698, 668 cm^{-1} ; HRMS (MM: ESI-APCI+) m/z calc'd for $\text{C}_{43}\text{H}_{38}\text{N}_9\text{O}_3$ $[\text{M} + \text{H}]^+$: 728.3098; found: 728.3102.

4.1.11. (S)-1-benzyl-3-isobutyl-N-(4-methyl-3-(1-methyl-7-((6-methylpyridin-3-yl)amino)-2-oxo-1,4-dihydropyrimido[4,5-d]pyrimidin-3(2H)-yl)phenyl)-2-oxo-5-phenyl-2,3-dihydro-1H-benzo[e][1,4]diazepine-8-carboxamide (11b)

(Purity: 98%; HPLC); R_f : 0.35 (1:10 MeOH:CH₂Cl₂); $[\alpha]_{\text{D}}^{26} = -74.4$ (c 0.0941, MeOH); ^1H NMR (400 MHz, DMSO) δ 10.49 (s, 1H), 9.62 (s, 1H), 8.78 (d, $J=2.6$ Hz, 1H), 8.20 (d, $J=1.6$ Hz, 1H), 8.15 (s, 1H), 8.05 (dd, $J=8.4, 2.7$ Hz, 1H), 7.78 (d, $J=2.8$ Hz, 1H), 7.74 (dd, $J=8.2, 1.6$ Hz, 1H), 7.62–7.57 (m, 1H), 7.53–7.48 (m, 1H), 7.42 (dd, $J=8.3, 6.7$ Hz, 2H), 7.33–7.26 (m, 4H), 7.18 (d, $J=8.5$ Hz, 1H), 7.13–7.06 (m, 3H), 6.97–6.93 (m, 2H), 5.57 (d, $J=15.6$ Hz, 1H), 5.01 (d, $J=15.6$ Hz, 1H), 4.69 (d, $J=14.1$ Hz, 1H), 4.51 (d, $J=14.1$ Hz, 1H), 3.74–3.64 (m, 2H), 3.33 (s, 3H), 2.40 (s, 3H), 2.13 (s, 3H), 1.93–1.83 (m, 2H), 0.94 (d, $J=6.2$ Hz, 3H), 0.77 (d, $J=6.0$ Hz, 3H); ^{13}C NMR (101 MHz, DMSO) δ 169.16, 167.47, 164.31, 159.06, 157.14, 153.40, 152.29, 150.40, 141.62, 141.29, 140.10, 138.01, 137.67, 137.14, 134.83, 132.43, 131.18, 130.95, 130.65, 129.73, 129.12, 128.53, 128.43, 127.28, 127.16, 126.52, 123.83, 122.69, 122.42, 119.98, 119.45, 103.08, 61.40, 49.11, 46.76, 28.36, 24.42, 23.41, 23.28, 22.08, 16.89; IR (Neat) 3285, 3031, 2952, 2867, 1661, 1597, 1576, 1530, 1507, 1491, 1466, 1408, 1319, 1293, 1231, 1185, 1143, 1119, 1078, 1029, 991, 908, 824, 784, 737, 696, 553, 518, 461, 411 cm^{-1} ; HRMS (MM: ESI-APCI+) m/z calc'd for $\text{C}_{47}\text{H}_{46}\text{N}_9\text{O}_3$ $[\text{M} + \text{H}]^+$: 784.3724; found: 784.3715.

4.1.12. (S)-3-methyl-N-(4-methyl-3-(1-methyl-7-((6-methylpyridin-3-yl)amino)-2-oxo-1,4-dihydropyrimido[4,5-d]pyrimidin-3(2H)-yl)phenyl)-2-oxo-5-phenyl-2,3-dihydro-1H-benzo[e][1,4]diazepine-8-carboxamide (11c)

(Purity: 97%; HPLC); R_f : 0.35 (1:10 MeOH:CH₂Cl₂); $[\alpha]_{\text{D}}^{26} = +40.5$ (c 0.124, MeOH); ^1H NMR (400 MHz, DMSO) δ 10.76 (s, 1H), 10.53 (s, 1H), 9.63 (s, 1H), 8.79 (d, $J=2.6$ Hz, 1H), 8.16 (d, $J=1.4$ Hz, 1H), 8.05 (dd, $J=8.4, 2.7$ Hz, 1H), 7.84 (t, $J=2.1$ Hz, 1H), 7.78 (d, $J=1.7$ Hz, 1H), 7.72 (dd, $J=8.2, 1.7$ Hz, 1H), 7.62 (dd, $J=8.3, 2.2$ Hz, 1H), 7.49 (dt, $J=7.0, 2.4$ Hz, 3H), 7.48–7.38 (m, 4H), 7.31 (d, $J=8.5$ Hz, 1H), 7.17 (d, $J=8.5$ Hz, 1H), 4.71 (d, $J=14.0$ Hz, 1H), 4.53 (d, $J=14.0$ Hz, 1H), 3.70 (q, $J=6.3$ Hz, 1H), 3.34 (s, 3H), 2.40 (s, 3H), 2.13 (s, 3H), 1.55 (d, $J=6.4$ Hz, 3H); ^{13}C NMR (101 MHz, DMSO) δ 171.34, 167.14, 164.49, 158.97, 157.04, 153.28, 152.13, 150.25, 141.19, 140.04, 139.39, 138.62, 137.76, 137.65, 134.73, 130.90, 130.80, 130.66, 130.35, 129.31, 128.93, 128.33, 126.29, 122.50, 121.26, 120.73, 119.68, 119.11, 102.97, 58.67, 46.67, 28.26, 23.23, 17.25, 16.82; IR (Neat) 3268, 3055, 2930, 2854, 1381, 1600, 1576, 1534, 1508, 1446, 1412, 1321, 1294, 1234, 1216, 1187, 1145, 1120, 1031, 949, 844, 784, 735, 698, 657, 557, 457 cm^{-1} ; HRMS (MM: ESI-

APCI+) m/z calc'd for $\text{C}_{37}\text{H}_{33}\text{N}_9\text{O}_3\text{Na}$ $[\text{M} + \text{Na}]^+$: 674.2604; found: 674.2606.

4.1.13. (S)-1-benzyl-3-methyl-N-(4-methyl-3-(1-methyl-7-((6-methylpyridin-3-yl)amino)-2-oxo-1,4-dihydropyrimido[4,5-d]pyrimidin-3(2H)-yl)phenyl)-2-oxo-5-phenyl-2,3-dihydro-1H-benzo[e][1,4]diazepine-8-carboxamide (11d)

(Purity: 97%; HPLC); R_f : 0.35 (1:10 MeOH:CH₂Cl₂); $[\alpha]_{\text{D}}^{30} = -3.70$ (c 0.172, MeOH); ^1H NMR (600 MHz, DMSO) δ 10.47 (s, 1H), 9.64 (s, 1H), 8.80 (d, $J=2.7$ Hz, 1H), 8.21 (d, $J=1.7$ Hz, 1H), 8.16 (s, 1H), 8.06 (dd, $J=8.4, 2.7$ Hz, 1H), 7.81 (dd, $J=4.7, 2.2$ Hz, 1H), 7.75 (dd, $J=8.1, 1.7$ Hz, 1H), 7.61 (ddd, $J=7.3, 4.6, 2.1$ Hz, 1H), 7.51 (t, $J=7.4$ Hz, 1H), 7.42 (t, $J=7.6$ Hz, 2H), 7.31 (dq, $J=6.7, 2.4, 1.6$ Hz, 4H), 7.18 (d, $J=8.5$ Hz, 1H), 7.15–7.08 (m, 3H), 7.00–6.95 (m, 2H), 5.58 (d, $J=15.6$ Hz, 1H), 5.04 (d, $J=15.6$ Hz, 1H), 4.70 (d, $J=14.0$ Hz, 1H), 4.53 (d, $J=14.0$ Hz, 1H), 3.86 (q, $J=6.2$ Hz, 1H), 3.34 (s, 3H), 2.41 (s, 3H), 2.14 (s, 3H), 1.61 (d, $J=6.3$ Hz, 3H); ^{13}C NMR (151 MHz, DMSO) δ 169.71, 167.06, 164.08, 158.93, 157.02, 153.24, 152.11, 150.17, 141.48, 141.18, 139.94, 137.86, 137.59, 137.45, 137.08, 134.72, 132.49, 130.96, 130.78, 130.44, 129.61, 129.00, 128.38, 128.25, 127.10, 127.04, 126.29, 123.54, 122.49, 122.28, 119.79, 119.29, 102.95, 58.37, 53.60, 48.93, 46.63, 41.84, 28.23, 23.18, 18.08, 17.48, 16.79, 16.72; IR (Neat) 3301, 2918, 2850, 1725, 1670, 1598, 1532, 1507, 1494, 1446, 1411, 1377, 1290, 1263, 1187, 1144, 1120, 1028, 963, 895, 822, 805, 785, 733, 698, 660, 555, 504, 460 cm^{-1} ; HRMS (MM: ESI-APCI+) m/z calc'd for $\text{C}_{44}\text{H}_{39}\text{N}_9\text{O}_3\text{Na}$ $[\text{M} + \text{Na}]^+$: 764.3074; found: 764.3049.

4.1.14. (R)-3-((R)-s-butyl)-N-(4-methyl-3-(1-methyl-7-((6-methylpyridin-3-yl)amino)-2-oxo-1,4-dihydropyrimido[4,5-d]pyrimidin-3(2H)-yl)phenyl)-2-oxo-5-phenyl-2,3-dihydro-1H-benzo[e][1,4]diazepine-8-carboxamide (11e)

(Purity: 96%; HPLC); R_f : 0.35 (1:10 MeOH:CH₂Cl₂); $[\alpha]_{\text{D}}^{28} = -26.2$ (c 0.0765, MeOH); ^1H NMR (400 MHz, DMSO) δ 10.78 (s, 1H), 10.53 (s, 1H), 9.64 (s, 1H), 8.80 (d, $J=2.7$ Hz, 1H), 8.16 (d, $J=1.7$ Hz, 1H), 8.05 (dd, $J=8.5, 2.7$ Hz, 1H), 7.85 (dd, $J=4.5, 2.2$ Hz, 1H), 7.79 (d, $J=1.7$ Hz, 1H), 7.72 (dd, $J=8.2, 1.7$ Hz, 1H), 7.62 (dd, $J=8.3, 2.2$ Hz, 1H), 7.54–7.41 (m, 6H), 7.31 (d, $J=8.4$ Hz, 1H), 7.18 (d, $J=8.5$ Hz, 1H), 4.72 (d, $J=13.9$ Hz, 1H), 4.53 (d, $J=14.0$ Hz, 1H), 3.34 (s, 3H), 3.13 (d, $J=9.5$ Hz, 1H), 2.41 (s, 3H), 2.14 (s, 3H), 2.00–1.90 (m, 1H), 1.31–1.21 (m, 2H), 0.97 (d, $J=6.6$ Hz, 3H), 0.91 (t, $J=7.4$ Hz, 3H); ^{13}C NMR (101 MHz, DMSO) δ 169.69, 167.45, 164.96, 159.43, 157.49, 154.35, 153.76, 152.57, 150.69, 141.65, 140.52, 139.77, 139.17, 138.24, 135.18, 131.33, 131.25, 131.13, 130.86, 129.77, 129.12, 128.84, 126.71, 122.92, 121.91, 121.09, 119.53, 103.43, 47.12, 40.63, 40.43, 40.22, 40.01, 39.80, 39.59, 39.38, 35.04, 28.71, 24.97, 23.70, 17.28, 16.53, 11.24; IR (Neat) 3239, 2957, 2924, 2854, 1688, 1658, 1600, 1577, 1534, 1508, 1494, 1465, 1412, 1321, 1296, 1231, 1188, 1145, 1120, 1033, 842, 785, 738, 698, 658, 558, 411 cm^{-1} ; HRMS (MM: ESI-APCI+) m/z calc'd for $\text{C}_{40}\text{H}_{39}\text{N}_9\text{O}_3\text{Na}$ $[\text{M} + \text{Na}]^+$: 716.3074; found: 716.3068.

4.1.15. (R)-N-(1-(((R)-1-(dimethylamino)-4-methyl-1-oxopentan-2-yl)amino)-2-methyl-1-oxopropan-2-yl)-1-((4-methyl-3-(1-methyl-7-((6-methylpyridin-3-yl)amino)-2-oxo-1,4-dihydropyrimido[4,5-d]pyrimidin-3(2H)-yl)benzoyl)-D-valyl)pyrrolidine-2-carboxamide (7c)

(Due to the distinct presence of rotameric isomers, the ^1H NMR and ^{13}C NMR contained extra peaks. See the attached spectrum in the supporting information) (Purity: 95%; HPLC); R_f : 0.35 (1:10 MeOH:CH₂Cl₂); $[\alpha]_{\text{D}}^{27} = +48.6$ (c 0.0410, MeOH); ^1H NMR

(400 MHz, DMSO) δ 9.64 (s, 1H), 8.79 (d, $J=2.7$ Hz, 1H), 8.42 (d, $J=8.0$ Hz, 1H), 8.14 (s, 1H), 8.05 (dd, $J=8.5, 2.7$ Hz, 1H), 8.00 (s, 1H), 7.93 (dd, $J=22.4, 1.8$ Hz, 1H), 7.87–7.77 (m, 1H), 7.40 (d, $J=8.0$ Hz, 1H), 7.27 (d, $J=8.5$ Hz, 1H), 7.17 (d, $J=8.5$ Hz, 1H), 4.86–4.66 (m, 2H), 4.56–4.44 (m, 2H), 4.28 (dd, $J=7.8, 4.8$ Hz, 1H), 3.89 (d, $J=9.6$ Hz, 1H), 3.63 (t, $J=8.2$ Hz, 1H), 3.32 (s, 3H), 2.98 (s, 3H), 2.78 (s, 3H), 2.40 (s, 3H), 2.20 (s, 3H), 2.15 (d, $J=23.1$ Hz, 1H), 2.07–1.91 (m, 2H), 1.86 (q, $J=5.6$ Hz, 2H), 1.50 (dq, $J=11.4, 5.7, 5.1$ Hz, 1H), 1.46–1.40 (m, 1H), 1.40–1.37 (m, 1H), 1.35 (s, 3H), 1.30 (s, 3H), 1.27–1.23 (m, 1H), 1.02–0.92 (m, 6H), 0.85 (dd, $J=11.2, 6.3$ Hz, 6H); ^{13}C NMR (101 MHz, DMSO) δ 173.25, 171.11, 170.96, 170.19, 170.14, 165.56, 165.39, 158.93, 156.93, 153.29, 153.22, 152.17, 152.12, 150.23, 141.10, 141.05, 140.04, 139.26, 134.68, 132.84, 132.74, 130.62, 126.84, 126.78, 126.56, 126.50, 126.24, 122.46, 102.91, 59.92, 59.88, 56.76, 55.99, 47.32, 46.69, 46.57, 40.91, 36.41, 35.13, 29.87, 28.88, 28.21, 25.41, 25.38, 24.70, 24.68, 24.59, 24.07, 23.23, 22.99, 22.97, 21.94, 21.92, 19.14, 19.06, 19.01, 17.28, 17.26; IR (Neat) 3300, 2959, 1632, 1607, 1530, 1496, 1411, 1332, 1240, 1174, 733 cm^{-1} ; IR (Neat) 3293, 2958, 1630, 1607, 1529, 1494, 1413, 1333, 1290, 1234, 1142, 1114, 1033, 845, 787, 735 cm^{-1} ; HRMS (MM: ESI-APCI+) m/z calc'd for $\text{C}_{43}\text{H}_{60}\text{N}_{11}\text{O}_6$ $[\text{M} + \text{H}]^+$: 826.4728; found: 826.4733.

4.1.16. (S)-N-(1-(((S)-1-(dimethylamino)-4-methyl-1-oxopentan-2-yl)carbamoyl)cyclopropyl)-1-((4-methyl-3-(1-methyl-7-((6-methylpyridin-3-yl)amino)-2-oxo-1,4-dihydropyrimido[4,5-d]pyrimidin-3(2H)-yl)benzoyl)-L-valyl)pyrrolidine-2-carboxamide (7d)

(Due to the distinct presence of rotameric isomers, the ^1H NMR and ^{13}C NMR contained extra peaks. See the attached spectrum in the supporting information) (Purity: 98%; HPLC); R_f : 0.35 (1:10 MeOH: CH_2Cl_2); $[\alpha]_{\text{D}}^{27} = -18.9$ (c 0.0520, MeOH); ^1H NMR (400 MHz, DMSO) δ 9.64 (s, 1H), 8.79 (d, $J=2.6$ Hz, 1H), 8.74 (d, $J=2.1$ Hz, 1H), 8.42–8.36 (m, 1H), 8.14 (d, $J=2.9$ Hz, 1H), 8.05 (dd, $J=8.4, 2.7$ Hz, 1H), 7.93 (dd, $J=24.4, 1.8$ Hz, 1H), 7.84 (ddd, $J=8.1, 3.9, 1.8$ Hz, 1H), 7.41 (dd, $J=8.2, 3.5$ Hz, 2H), 7.18 (d, $J=8.5$ Hz, 1H), 4.84–4.71 (m, 2H), 4.58–4.47 (m, 2H), 4.13 (t, $J=7.1$ Hz, 1H), 3.97–3.87 (m, 1H), 3.68–3.57 (m, 1H), 3.33 (s, 3H), 3.00 (s, 3H), 2.77 (d, $J=3.0$ Hz, 3H), 2.40 (s, 3H), 2.20 (s, 3H), 2.07–1.95 (m, 2H), 1.89–1.71 (m, 2H), 1.57–1.45 (m, 2H), 1.43–1.34 (m, 1H), 1.33–1.12 (m, 3H), 0.96 (dd, $J=6.7$ Hz, 6H), 0.85–0.80 (m, 8H); ^{13}C NMR (101 MHz, DMSO) δ 173.14, 171.52, 171.02, 170.59, 170.53, 166.05, 165.89, 159.41, 157.42, 153.76, 153.69, 152.62, 152.59, 150.71, 141.61, 141.54, 140.51, 139.78, 135.16, 133.32, 133.21, 131.11, 127.31, 127.06, 126.91, 126.72, 122.94, 103.40, 60.61, 60.56, 57.15, 57.09, 47.89, 47.53, 47.04, 41.32, 36.98, 35.64, 34.10, 30.30, 29.36, 28.68, 25.28, 24.56, 24.54, 23.70, 23.33, 23.29, 22.50, 22.46, 19.74, 19.69, 19.42, 19.29, 17.76, 16.86, 16.21; IR (Neat) 3296, 2957, 2871, 1627, 1606, 1575, 1525, 1492, 1410, 1332, 1290, 1233, 1195, 1140, 1112, 1071, 1034, 938, 831, 786, 731, 700, 621, 559, 516, 457 cm^{-1} ; HRMS (MM: ESI-APCI+) m/z calc'd for $\text{C}_{43}\text{H}_{57}\text{N}_{11}\text{O}_6\text{Na}$ $[\text{M} + \text{Na}]^+$: 846.4391; found: 846.4385.

4.1.17. (R)-N-(1-(((S)-1-(dimethylamino)-4-methyl-1-oxopentan-2-yl)carbamoyl)cyclopropyl)-1-((4-methyl-3-(1-methyl-7-((6-methylpyridin-3-yl)amino)-2-oxo-1,4-dihydropyrimido[4,5-d]pyrimidin-3(2H)-yl)benzoyl)-L-valyl)pyrrolidine-2-carboxamide (7e)

(Due to the distinct presence of rotameric isomers, the ^1H NMR and ^{13}C NMR contained extra peaks. See the attached spectrum in the supporting information) (Purity: 98%; HPLC); R_f : 0.35 (1:10 MeOH: CH_2Cl_2); $[\alpha]_{\text{D}}^{31} = -150.0$ (c 0.0530, MeOH); ^1H NMR

(600 MHz, DMSO) δ 9.63 (d, $J=8.3$ Hz, 1H), 8.79 (t, $J=2.8$ Hz, 1H), 8.65–8.42 (m, 2H), 8.10 (d, $J=21.1$ Hz, 1H), 8.05 (dd, $J=8.5, 2.8$ Hz, 1H), 7.90–7.81 (m, 2H), 7.80–7.73 (m, 1H), 7.36 (dd, $J=15.5, 8.0$ Hz, 1H), 7.18 (d, $J=8.5$ Hz, 1H), 4.75 (td, $J=19.3, 17.8, 10.8$ Hz, 2H), 4.63 (dt, $J=25.8, 9.0$ Hz, 1H), 4.40 (dd, $J=87.9, 14.0$ Hz, 1H), 4.23–4.17 (m, 1H), 3.68 (d, $J=6.9$ Hz, 2H), 3.33 (s, 3H), 3.00 (d, $J=34.1$ Hz, 3H), 2.60 (d, $J=42.9$ Hz, 3H), 2.40 (s, 3H), 2.17 (d, $J=14.0$ Hz, 4H), 2.11–2.03 (m, 1H), 1.97 (m, 1H), 1.86 (m, 1H), 1.79 (m, 1H), 1.72 (m, 1H), 1.65 (m, 1H), 1.39 (m, 1H), 1.25–1.05 (m, 3H), 0.94 (d, $J=7.4$ Hz, 6H), 0.86 (m, 6H), 0.81–0.74 (m, 2H); ^{13}C NMR (151 MHz, DMSO) δ 173.34, 173.14, 172.13, 172.08, 171.12, 170.99, 170.53, 170.49, 167.06, 166.18, 159.29, 159.27, 157.29, 157.26, 153.66, 152.47, 152.38, 150.59, 141.43, 141.32, 140.41, 139.60, 139.14, 135.06, 134.04, 133.30, 130.83, 130.65, 127.00, 126.61, 122.82, 103.37, 60.79, 60.69, 57.03, 56.85, 47.64, 47.32, 47.23, 46.89, 46.69, 40.96, 40.69, 36.93, 35.53, 35.34, 34.05, 30.21, 28.87, 28.77, 28.58, 24.98, 24.95, 24.32, 23.61, 23.59, 23.54, 23.49, 21.82, 19.64, 19.57, 19.00, 18.92, 17.72, 17.70, 16.27, 16.20, 16.00, 15.95; IR (Neat) 3294, 2957, 2923, 2853, 2360, 2340, 2628, 1574, 1533, 1496, 1414, 1333, 1294, 1236, 1149, 1115, 1026, 1007, 821, 753 cm^{-1} ; HRMS (MM: ESI-APCI+) m/z calc'd for $\text{C}_{43}\text{H}_{58}\text{N}_{11}\text{O}_6$ $[\text{M} + \text{H}]^+$: 824.4572; found: 824.4574.

4.1.18. (S)-N-(1-(((S)-1-(dimethylamino)-4-methyl-1-oxopentan-2-yl)carbamoyl)cyclobutyl)-1-((4-methyl-3-(1-methyl-7-((6-methylpyridin-3-yl)amino)-2-oxo-1,4-dihydropyrimido[4,5-d]pyrimidin-3(2H)-yl)benzoyl)-L-valyl)pyrrolidine-2-carboxamide (7f)

(Due to the distinct presence of rotameric isomers, the ^1H NMR and ^{13}C NMR contained extra peaks. See the attached spectrum in the supporting information) (Purity: 96%; HPLC); R_f : 0.35 (1:10 MeOH: CH_2Cl_2); $[\alpha]_{\text{D}}^{31} = -56.7$ (c 0.0530, MeOH); ^1H NMR (400 MHz, DMSO) δ 9.68 (s, 1H), 8.81 (d, $J=2.7$ Hz, 1H), 8.49 (s, 1H), 8.44 (d, $J=8.1$ Hz, 1H), 8.15 (s, 1H), 8.07 (dd, $J=8.5, 2.7$ Hz, 1H), 7.94 (dd, $J=23.1, 1.8$ Hz, 1H), 7.88–7.78 (m, 1H), 7.40 (d, $J=8.1$ Hz, 1H), 7.19 (dd, $J=8.7, 5.2$ Hz, 2H), 4.84–4.71 (m, 2H), 4.56–4.48 (m, 2H), 4.26 (dd, $J=7.9, 5.3$ Hz, 1H), 3.89 (ddt, $J=13.0, 8.8, 4.2$ Hz, 1H), 3.64 (dq, $J=10.9, 5.4, 3.9$ Hz, 1H), 3.33 (d, $J=2.4$ Hz, 3H), 2.99 (s, 3H), 2.78 (d, $J=3.2$ Hz, 3H), 2.41 (s, 3H), 2.40–2.33 (m, 1H), 2.20 (s, 3H), 2.17 (dd, $J=8.1, 5.4$ Hz, 1H), 2.12–1.92 (m, 4H), 1.84 (ddt, $J=20.9, 14.2, 7.0$ Hz, 4H), 1.53–1.40 (m, 2H), 1.38–1.31 (m, 1H), 1.26 (t, $J=6.1$ Hz, 1H), 0.99–0.93 (m, 6H), 0.86 (dd, $J=16.6, 6.2$ Hz, 6H); ^{13}C NMR (101 MHz, DMSO) δ 172.72, 171.72, 171.59, 170.64, 170.59, 166.04, 165.87, 159.37, 157.42, 153.75, 153.69, 152.63, 152.58, 150.52, 141.58, 141.53, 140.14, 139.74, 135.27, 133.32, 133.22, 131.09, 127.32, 127.26, 127.04, 126.99, 123.10, 103.45, 60.26, 60.22, 58.87, 57.20, 54.08, 47.81, 47.04, 41.63, 36.89, 35.59, 31.13, 30.79, 30.33, 29.44, 28.68, 25.11, 25.09, 24.52, 23.52, 23.48, 23.46, 22.35, 22.33, 19.67, 19.65, 19.45, 19.40, 18.55, 17.74, 17.20, 15.82; IR (Neat) 3288, 2955, 2360, 2339, 1606, 1527, 1493, 1411, 1331, 1288, 1233, 1196, 1140, 1113, 1033, 953, 843, 787, 732 cm^{-1} ; HRMS (MM: ESI-APCI+) m/z calc'd for $\text{C}_{44}\text{H}_{60}\text{N}_{11}\text{O}_6$ $[\text{M} + \text{H}]^+$: 838.4728; found: 838.4726.

4.1.19. (S)-N-(2-(((S)-1-(dimethylamino)-4-methyl-1-oxopentan-2-yl)amino)-2-oxoethyl)-1-((4-methyl-3-(1-methyl-7-((6-methylpyridin-3-yl)amino)-2-oxo-1,4-dihydropyrimido[4,5-d]pyrimidin-3(2H)-yl)benzoyl)-L-valyl)pyrrolidine-2-carboxamide (7g)

(Due to the distinct presence of rotameric isomers, the ^1H NMR and ^{13}C NMR contained extra peaks. See the attached spectrum in the supporting information) (Purity: 95%; HPLC); R_f : 0.35 (1:10 MeOH: CH_2Cl_2); $[\alpha]_{\text{D}}^{30} = -12.1$ (c 0.0820, MeOH); ^1H NMR

(600 MHz, DMSO) δ 9.75 (s, 1H), 8.85 (s, 1H), 8.45 (dd, $J=8.2$, 3.5 Hz, 1H), 8.19 (t, $J=5.1$ Hz, 1H), 8.16 (s, 1H), 8.13–8.07 (m, 1H), 7.93 (d, $J=28.2$ Hz, 1H), 7.86 (d, $J=8.5$ Hz, 1H), 7.83 (t, $J=8.5$ Hz, 1H), 7.40 (d, $J=7.9$ Hz, 1H), 7.26 (d, $J=8.5$ Hz, 1H), 4.81–4.75 (m, 2H), 4.52 (dt, $J=17.3$, 6.5 Hz, 2H), 4.32 (dd, $J=8.0$, 4.6 Hz, 1H), 3.90 (dt, $J=10.1$, 5.8 Hz, 1H), 3.71–3.65 (m, 3H), 3.34 (d, $J=3.2$ Hz, 3H), 3.02 (s, 3H), 2.80 (s, 3H), 2.43 (s, 3H), 2.20 (s, 3H), 2.17 (t, $J=7.3$ Hz, 1H), 2.07–2.03 (m, 1H), 1.98–1.94 (m, 1H), 1.85 (t, $J=6.0$ Hz, 1H), 1.55–1.51 (m, 1H), 1.41 (s, 1H), 1.27–1.25 (m, 2H), 0.99–0.93 (m, 6H), 0.86 (d, $J=6.6$ Hz, 6H); ^{13}C NMR (151 MHz, DMSO) δ 172.22, 171.61, 170.48, 170.43, 168.86, 168.62, 165.86, 165.71, 161.57, 159.16, 157.34, 153.60, 152.50, 152.44, 149.97, 141.44, 141.39, 139.62, 139.10, 135.44, 133.18, 133.08, 130.98, 127.56, 127.21, 126.89, 123.46, 103.52, 63.15, 61.03, 60.28, 59.96, 59.92, 57.12, 57.09, 53.93, 47.81, 47.61, 46.92, 46.86, 42.16, 41.07, 36.88, 35.53, 30.84, 30.21, 30.18, 29.65, 29.40, 28.60, 25.11, 24.88, 24.86, 24.48, 23.46, 23.44, 23.38, 23.37, 23.03, 22.04, 22.02, 22.00, 19.53, 19.49, 19.44, 19.40, 19.34, 19.10, 18.43, 17.82, 17.65, 17.63, 17.09, 12.83; IR (Neat) 3291, 2958, 1739, 1630, 1574, 1533, 1496, 1415, 1336, 1291, 1232, 1142, 1115, 1033, 844, 787, 736 cm^{-1} ; HRMS (MM: ESI-APCI+) m/z calc'd for $\text{C}_{41}\text{H}_{56}\text{N}_{11}\text{O}_6$ $[\text{M} + \text{H}]^+$: 798.4415; found: 798.4420.

4.1.20. (R)-N-(2-(((S)-1-(dimethylamino)-4-methyl-1-oxopentan-2-yl)amino)-2-oxoethyl)-1-((4-methyl-3-(1-methyl-7-((6-methylpyridin-3-yl)amino)-2-oxo-1,4-dihydropyrimido[4,5-d]pyrimidin-3(2H)-yl)benzoyl)-L-valyl)pyrrolidine-2-carboxamide (7h)

(Due to the distinct presence of rotameric isomers, the ^1H NMR and ^{13}C NMR contained extra peaks. See the attached spectrum in the supporting information) (Purity: 98%; HPLC); R_f : 0.35 (1:10 MeOH:CH₂Cl₂); $[\alpha]_{\text{D}}^{32} = -51.0$ (c 0.0590, MeOH); ^1H NMR (600 MHz, DMSO) δ 9.65 (s, 1H), 8.79 (s, 1H), 8.48 (dd, $J=16.2$, 8.2 Hz, 1H), 8.14 (d, $J=7.4$ Hz, 1H), 8.05 (dd, $J=8.5$, 2.5 Hz, 2H), 7.92–7.88 (m, 1H), 7.86 (dd, $J=8.5$, 2.0 Hz, 1H), 7.82–7.80 (m, 1H), 7.39–7.37 (m, 1H), 7.18 (s, 1H), 4.78–4.75 (m, 2H), 4.57–4.55 (m, 1H), 4.52–4.48 (m, 1H), 4.45 (d, $J=14.0$ Hz, 1H), 4.31 (dt, $J=8.2$, 4.0 Hz, 1H), 3.85–3.77 (m, 2H), 3.67–3.64 (m, 2H), 3.33 (s, 3H), 3.00 (d, $J=11.9$ Hz, 3H), 2.73 (d, $J=11.7$ Hz, 3H), 2.40 (s, 3H), 2.20 (d, $J=3.5$ Hz, 3H), 1.99 (t, $J=6.3$ Hz, 2H), 1.88 (dt, $J=8.6$, 5.1 Hz, 2H), 1.61–1.55 (m, 2H), 1.35 (ddd, $J=8.9$, 4.4, 2.1 Hz, 1H), 0.95 (d, $J=6.7$ Hz, 3H), 0.93 (d, $J=6.6$ Hz, 3H), 0.85 (s, 6H); ^{13}C NMR (151 MHz, DMSO) δ 172.21, 172.14, 171.89, 171.73, 170.52, 168.66, 168.61, 168.46, 166.39, 166.16, 159.29, 157.29, 153.63, 152.48, 152.41, 150.60, 150.58, 141.44, 141.40, 140.39, 139.67, 139.53, 135.06, 133.33, 133.12, 130.92, 130.86, 127.19, 126.96, 126.79, 126.59, 122.83, 103.32, 60.36, 57.17, 57.14, 47.50, 46.93, 46.88, 46.82, 42.32, 42.28, 41.20, 40.90, 40.79, 40.42, 36.88, 35.54, 35.52, 35.48, 31.06, 30.08, 30.06, 29.49, 29.43, 28.58, 24.55, 24.51, 24.42, 24.39, 23.60, 23.50, 21.95, 21.79, 19.54, 19.52, 19.12, 17.71, 17.68; IR (Neat) 3290, 2957, 2361, 2340, 1629, 1608, 1574, 1533, 1494, 1412, 1333, 1289, 1235, 1142, 1115, 1028, 840, 787, 736 cm^{-1} ; HRMS (MM: ESI-APCI+) m/z calc'd for $\text{C}_{41}\text{H}_{56}\text{N}_{11}\text{O}_6$ $[\text{M} + \text{H}]^+$: 798.4415; found: 798.4425.

4.1.21. (S)-N-(((S)-1-(((S)-1-(dimethylamino)-4-methyl-1-oxopentan-2-yl)amino)-1-oxo-3-phenylpropan-2-yl)-1-((4-methyl-3-(1-methyl-7-((6-methylpyridin-3-yl)amino)-2-oxo-1,4-dihydropyrimido[4,5-d]pyrimidin-3(2H)-yl)benzoyl)-L-valyl)pyrrolidine-2-carboxamide (7i)

(Due to the distinct presence of rotameric isomers, the ^1H NMR and ^{13}C NMR contained extra peaks. See the attached spectrum in the supporting information) (Purity: 95%; HPLC); R_f : 0.35 (1:10

MeOH:CH₂Cl₂); $[\alpha]_{\text{D}}^{29} = -15.5$ (c 0.130, MeOH); ^1H NMR (400 MHz, DMSO) δ 9.64 (d, $J=4.8$ Hz, 1H), 8.79 (d, $J=2.6$ Hz, 1H), 8.51 (d, $J=8.1$ Hz, 1H), 8.15 (d, $J=4.8$ Hz, 1H), 8.09–7.97 (m, 2H), 7.97–7.87 (m, 2H), 7.81 (td, $J=7.7$, 1.9 Hz, 1H), 7.46–7.33 (m, 1H), 7.27–7.09 (m, 6H), 4.76 (ddd, $J=17.7$, 14.0, 9.9 Hz, 2H), 4.56–4.31 (m, 4H), 3.85 (dq, $J=11.9$, 6.9, 5.9 Hz, 1H), 3.62 (dt, $J=11.8$, 6.1 Hz, 1H), 3.32 (s, 3H), 3.02–2.95 (m, 1H), 2.93 (s, 3H), 2.91–2.82 (m, 1H), 2.80 (s, 3H), 2.40 (s, 3H), 2.20 (s, 3H), 2.15–2.08 (m, 1H), 1.97 (dt, $J=11.1$, 8.0 Hz, 1H), 1.83 (tt, $J=13.3$, 6.6 Hz, 2H), 1.54 (dq, $J=12.8$, 6.6 Hz, 1H), 1.39 (tdd, $J=13.7$, 9.0, 5.0 Hz, 2H), 1.18–1.09 (m, 1H), 1.03–0.90 (m, 6H), 0.91–0.72 (m, 6H); ^{13}C NMR (101 MHz, DMSO) δ 171.76, 171.56, 170.66, 170.61, 165.96, 165.82, 159.41, 157.42, 153.73, 152.65, 152.57, 150.70, 141.56, 141.51, 140.52, 139.71, 138.01, 135.16, 133.26, 133.18, 131.07, 129.74, 129.63, 128.42, 127.32, 127.04, 126.97, 126.72, 126.65, 122.93, 103.39, 59.83, 57.32, 54.09, 47.66, 47.05, 46.95, 37.68, 36.91, 35.63, 30.33, 30.29, 29.59, 28.69, 24.76, 24.47, 23.71, 23.57, 22.15, 19.63, 19.59, 17.77, 17.74, 17.61; IR (Neat) 3388, 3300, 2955, 2924, 2854, 1728, 1672, 1460, 1415, 1377, 1260, 1018, 952, 799, 705, 667, 609, 554, 533, 498, 469, 447, 411 cm^{-1} ; HRMS (MM: ESI-APCI+) m/z calc'd for $\text{C}_{48}\text{H}_{62}\text{N}_{11}\text{O}_6$ $[\text{M} + \text{H}]^+$: 888.4885; found: 888.4888.

4.1.22. (S)-N-(1-(((S)-1-(dimethylamino)-4-methyl-1-oxopentan-2-yl)amino)-2-methyl-1-oxopropan-2-yl)-1-((4-methyl-3-(1-methyl-7-((6-methylpyridin-3-yl)amino)-2-oxo-1,4-dihydropyrimido[4,5-d]pyrimidin-3(2H)-yl)benzoyl)-L-valyl)piperidine-2-carboxamide (7j)

(Due to the distinct presence of rotameric isomers, the ^1H NMR and ^{13}C NMR contained extra peaks. See the attached spectrum in the supporting information) (Purity: 96%; HPLC); R_f : 0.35 (1:10 MeOH:CH₂Cl₂); $[\alpha]_{\text{D}}^{31} = -14.2$ (c 0.0710, MeOH); ^1H NMR (600 MHz, DMSO) δ 9.65 (d, $J=3.2$ Hz, 2H), 8.79 (d, $J=2.7$ Hz, 2H), 8.75 (dd, $J=10.0$, 7.0 Hz, 1H), 8.47 (dd, $J=15.8$, 8.6 Hz, 1H), 8.18–8.13 (m, 2H), 8.08–8.03 (m, 3H), 7.99 (dd, $J=12.1$, 1.9 Hz, 1H), 7.94 (dd, $J=32.2$, 1.9 Hz, 1H), 7.88–7.83 (m, 1H), 7.81 (ddd, $J=7.2$, 4.8, 2.0 Hz, 1H), 7.65 (d, $J=4.2$ Hz, 1H), 7.46 (t, $J=9.0$ Hz, 1H), 7.40 (dq, $J=8.9$, 4.9, 3.7 Hz, 3H), 7.18 (d, $J=8.5$ Hz, 2H), 5.04 (q, $J=4.3$, 3.8 Hz, 1H), 4.93 (d, $J=3.2$ Hz, 1H), 4.87–4.76 (m, 4H), 4.73 (td, $J=9.6$, 5.3 Hz, 2H), 4.70–4.62 (m, 1H), 4.56–4.42 (m, 3H), 4.07 (t, $J=13.9$ Hz, 1H), 3.33 (d, $J=3.7$ Hz, 6H), 2.99–2.96 (m, 6H), 2.81–2.76 (m, 6H), 2.70 (q, $J=11.7$ Hz, 1H), 2.40 (s, 6H), 2.20 (d, $J=2.3$ Hz, 6H), 2.18–2.15 (m, 1H), 2.10 (d, $J=12.2$ Hz, 1H), 1.63–1.49 (m, 8H), 1.45 (p, $J=6.0$, 5.5 Hz, 3H), 1.42–1.40 (m, 6H), 1.39 (d, $J=5.3$ Hz, 1H), 1.37 (s, 3H), 1.34 (s, 3H), 1.31–1.17 (m, 4H), 0.98 (d, $J=6.8$ Hz, 3H), 0.93 (d, $J=6.7$ Hz, 3H), 0.90 (d, $J=6.6$ Hz, 3H), 0.86 (d, $J=6.5$ Hz, 3H), 0.83 (dd, $J=10.0$, 6.4 Hz, 6H), 0.70 (t, $J=6.3$ Hz, 3H); ^{13}C NMR (151 MHz, DMSO) δ 206.85, 173.70, 171.94, 171.89, 171.52, 171.44, 171.40, 171.32, 170.25, 169.31, 166.40, 166.22, 165.66, 165.49, 159.30, 159.29, 157.30, 153.59, 152.54, 152.47, 152.44, 152.39, 150.60, 150.59, 141.49, 141.47, 141.38, 140.39, 140.01, 139.63, 135.05, 133.26, 133.13, 132.45, 130.99, 127.06, 126.82, 126.61, 122.83, 103.30, 56.59, 56.54, 56.34, 56.15, 56.05, 55.26, 54.55, 52.46, 47.09, 47.06, 46.94, 43.56, 41.33, 36.77, 36.68, 35.49, 35.38, 31.06, 30.31, 30.24, 30.17, 28.58, 27.06, 26.91, 25.42, 25.31, 25.24, 25.11, 25.07, 25.04, 24.99, 24.35, 24.25, 23.59, 23.52, 22.08, 21.77, 21.73, 20.62, 20.33, 19.90, 19.87, 19.85, 19.82, 19.66, 18.94, 17.72, 17.67, 17.65, 17.63; IR (Neat) 3289, 2932, 1606, 1575, 1530, 1493, 1411, 1333, 1265, 1231, 1193, 1139, 1114, 1019, 952, 842, 787, 733 cm^{-1} ; HRMS (MM: ESI-APCI+) m/z calc'd for $\text{C}_{44}\text{H}_{62}\text{N}_{11}\text{O}_6$ $[\text{M} + \text{H}]^+$: 840.4885; found: 840.4897.

4.1.23. (S)-N-(1-(((S)-1-(dimethylamino)-4-methyl-1-oxopentan-2-yl)amino)-2-methyl-1-oxopropan-2-yl)-1-((4-methyl-3-(1-methyl-7-((6-methylpyridin-3-yl)amino)-2-oxo-1,4-dihydropyrimido[4,5-d]pyrimidin-3(2H)-yl)benzoyl)-L-valyl)azetidine-2-carboxamide (7k)

(Due to the distinct presence of rotameric isomers, the ^1H NMR and ^{13}C NMR contained extra peaks. See the attached spectrum in the supporting information) (Purity: 99%; HPLC); R_f : 0.35 (1:10 MeOH:CH₂Cl₂); $[\alpha]_D^{28} = -40.5$ (c 0.0220, MeOH); ^1H NMR (600 MHz, DMSO) δ 9.65 (s, 1H), 8.79 (d, $J = 2.6$ Hz, 1H), 8.54 (d, $J = 8.0$ Hz, 1H), 8.15 (d, $J = 4.2$ Hz, 1H), 8.10–8.03 (m, 2H), 7.97–7.89 (m, 1H), 7.82 (t, $J = 8.5$ Hz, 1H), 7.41 (d, $J = 7.9$ Hz, 1H), 7.34 (d, $J = 8.5$ Hz, 1H), 7.18 (d, $J = 8.5$ Hz, 1H), 4.78 (t, $J = 14.8$ Hz, 1H), 4.73 (td, $J = 9.1$, 4.8 Hz, 1H), 4.65 (dd, $J = 9.0$, 5.9 Hz, 1H), 4.52 (dd, $J = 14.0$, 5.7 Hz, 1H), 4.37–4.32 (m, 1H), 4.20–4.13 (m, 2H), 3.34 (d, $J = 3.9$ Hz, 3H), 2.99 (s, 3H), 2.80 (s, 3H), 2.41 (d, $J = 8.5$ Hz, 3H), 2.38 (d, $J = 8.5$ Hz, 1H), 2.20 (s, 3H), 2.17–2.07 (m, 2H), 1.53 (d, $J = 13.5$ Hz, 1H), 1.46–1.39 (m, 2H), 1.36 (s, 3H), 1.35 (s, 3H), 0.96 (dd, $J = 15.1$, 6.5 Hz, 6H), 0.86 (dd, $J = 16.2$, 6.5 Hz, 6H); ^{13}C NMR (151 MHz, DMSO) δ 173.39, 171.78, 171.63, 169.45, 165.93, 165.78, 159.30, 157.31, 153.66, 152.55, 150.60, 141.46, 140.41, 139.66, 135.04, 133.02, 130.99, 127.21, 126.89, 126.61, 122.83, 103.29, 63.15, 60.81, 56.35, 54.98, 54.94, 49.19, 47.12, 46.94, 41.18, 36.78, 35.52, 29.56, 28.59, 25.40, 25.39, 25.13, 25.12, 24.39, 23.60, 23.51, 22.04, 19.61, 19.38, 17.67, 17.64; IR (Neat) 3293, 2926, 1635, 1607, 1531, 1495, 1467, 1412, 1333, 1290, 1241, 1142, 1071, 845, 787, 734 cm⁻¹; HRMS (MM: ESI-APCI+) m/z calc'd for C₄₂H₅₈N₁₁O₆ [M + H]⁺: 812.4572; found: 812.4561.

4.1.24. (S)-N-(1-(((S)-1-(dimethylamino)-3-methyl-1-oxobutan-2-yl)amino)-2-methyl-1-oxopropan-2-yl)-1-((4-methyl-3-(1-methyl-7-((6-methylpyridin-3-yl)amino)-2-oxo-1,4-dihydropyrimido[4,5-d]pyrimidin-3(2H)-yl)benzoyl)-L-phenylalanyl)pyrrolidine-2-carboxamide (7l)

(Due to the distinct presence of rotameric isomers, the ^1H NMR and ^{13}C NMR contained extra peaks. See the attached spectrum in the supporting information) (Purity: 99%; HPLC); R_f : 0.35 (1:10 MeOH:CH₂Cl₂); $[\alpha]_D^{29} = -46.5$ (c 0.0667, MeOH); ^1H NMR (400 MHz, DMSO) δ 9.64 (s, 1H), 8.79 (d, $J = 2.6$ Hz, 1H), 8.42 (d, $J = 7.3$ Hz, 1H), 8.13 (s, 1H), 8.10 (s, 1H), 8.05 (dd, $J = 8.5$, 2.7 Hz, 1H), 7.96–7.88 (m, 1H), 7.85–7.78 (m, 1H), 7.41 (dd, $J = 10.6$, 8.0 Hz, 2H), 7.23 (dd, $J = 8.0$, 6.4 Hz, 2H), 7.20–7.14 (m, 4H), 4.88–4.71 (m, 2H), 4.49 (dd, $J = 14.0$, 8.9 Hz, 2H), 4.28 (t, $J = 6.4$ Hz, 1H), 3.91 (m, 1H), 3.67–3.56 (m, 1H), 3.33 (s, 3H), 2.96 (dd, $J = 13.4$, 7.9 Hz, 1H), 2.80 (m, 1H), 2.72 (s, 3H), 2.70 (d, $J = 2.1$ Hz, 3H), 2.40 (s, 3H), 2.19 (s, 3H), 2.17–2.08 (m, 1H), 2.08–1.90 (m, 2H), 1.83 (d, $J = 6.2$ Hz, 2H), 1.28 (d, $J = 17.4$ Hz, 6H), 0.93 (dd, $J = 11.5$, 6.6 Hz, 6H); ^{13}C NMR (101 MHz, DMSO) δ 173.58, 171.55, 170.73, 166.06, 159.41, 152.59, 150.72, 140.52, 139.71, 138.04, 135.15, 131.09, 129.75, 128.47, 126.77, 122.93, 103.40, 60.34, 57.27, 56.40, 50.48, 47.82, 47.03, 38.23, 36.77, 35.56, 30.27, 29.33, 28.67, 25.88, 25.11, 23.70, 19.53, 19.48, 17.74; IR (Neat) 3298, 2924, 1628, 1605, 1576, 1528, 1493, 1448, 1411, 1332, 1288, 1294, 1235, 1194, 1142, 1112, 1075, 1031, 943, 830, 787, 732, 700, 623, 548, 514, 480, 458 cm⁻¹; HRMS (MM: ESI-APCI+) m/z calc'd for C₄₆H₅₈N₁₁O₆ [M + H]⁺: 860.4572; found: 860.4589.

4.1.25. (S)-N-(1-(((S)-1-(dimethylamino)-3-methyl-1-oxobutan-2-yl)amino)-2-methyl-1-oxopropan-2-yl)-1-((4-methyl-3-(1-methyl-7-((6-methylpyridin-3-yl)amino)-2-oxo-1,4-dihydropyrimido[4,5-d]pyrimidin-3(2H)-yl)benzoyl)-L-alanyl)pyrrolidine-2-carboxamide (7m)

(Due to the distinct presence of rotameric isomers, the ^1H NMR and ^{13}C NMR contained extra peaks. See the attached spectrum in

the supporting information) (Purity: 96%; HPLC); R_f : 0.35 (1:10 MeOH:CH₂Cl₂); $[\alpha]_D^{30} = -42.0$ (c 0.0667, MeOH); ^1H NMR (400 MHz, DMSO) δ 9.62 (s, 1H), 8.79 (d, $J = 2.6$ Hz, 1H), 8.41 (d, $J = 8.0$ Hz, 1H), 8.15 (d, $J = 4.6$ Hz, 2H), 8.05 (dd, $J = 8.5$, 2.7 Hz, 1H), 7.95–7.88 (m, 1H), 7.85–7.78 (m, 1H), 7.40 (d, $J = 7.9$ Hz, 1H), 7.37 (d, $J = 4.8$ Hz, 1H), 7.24 (d, $J = 7.6$ Hz, 1H), 7.18 (d, $J = 8.4$ Hz, 1H), 4.78 (dd, $J = 14.0$, 6.5 Hz, 1H), 4.63 (t, $J = 7.0$ Hz, 1H), 4.54–4.48 (m, 1H), 4.46 (d, $J = 7.6$ Hz, 1H), 4.28 (dd, $J = 7.6$, 5.6 Hz, 1H), 3.96 (d, $J = 9.9$ Hz, 1H), 3.62 (d, $J = 8.8$ Hz, 1H), 3.51 (d, $J = 24.5$ Hz, 2H), 3.33 (s, 3H), 2.97 (d, $J = 1.7$ Hz, 3H), 2.78 (s, 3H), 2.41 (s, 3H), 2.20 (s, 3H), 2.17–2.10 (m, 1H), 2.06–1.91 (m, 2H), 1.82 (td, $J = 11.9$, 11.4, 6.3 Hz, 2H), 1.34 (s, 3H), 1.28 (s, 3H), 1.14 (d, $J = 6.8$ Hz, 3H), 0.95 (t, $J = 6.5$ Hz, 6H); ^{13}C NMR (101 MHz, DMSO) δ 173.38, 171.98, 171.96, 171.61, 170.61, 166.06, 159.41, 157.43, 152.65, 150.72, 141.53, 140.52, 139.72, 135.15, 133.30, 133.04, 132.85, 131.09, 129.33, 129.03, 127.23, 127.00, 126.75, 122.93, 103.41, 60.30, 57.38, 56.33, 51.77, 47.87, 47.05, 45.10, 36.84, 35.65, 31.15, 30.20, 29.40, 28.68, 26.48, 25.15, 24.61, 23.69, 19.63, 19.42, 17.74; IR (Neat) 3294, 2962, 2965, 1735, 1632, 1609, 1575, 1531, 1495, 1414, 1333, 1291, 1236, 1196, 1143, 1114, 1034, 947, 832, 787, 740, 699, 625, 598, 513, 452, 418 cm⁻¹; HRMS (MM: ESI-APCI+) m/z calc'd for C₄₀H₅₄N₁₁O₆ [M + H]⁺: 784.4259; found: 784.4248.

4.1.26. (S)-N-(1-(((S)-1-(dimethylamino)-3-methyl-1-oxobutan-2-yl)amino)-2-methyl-1-oxopropan-2-yl)-1-((4-methyl-3-(1-methyl-7-((6-methylpyridin-3-yl)amino)-2-oxo-1,4-dihydropyrimido[4,5-d]pyrimidin-3(2H)-yl)benzoyl)-L-valyl)pyrrolidine-2-carboxamide (7n)

(Due to the distinct presence of rotameric isomers, the ^1H NMR and ^{13}C NMR contained extra peaks. See the attached spectrum in the supporting information) (Purity: 96%; HPLC); R_f : 0.35 (1:10 MeOH:CH₂Cl₂); $[\alpha]_D^{29} = -90.7$ (c 0.0882, MeOH); ^1H NMR (400 MHz, DMSO) δ 9.64 (s, 1H), 8.79 (d, $J = 2.7$ Hz, 1H), 8.48–8.41 (m, 1H), 8.15 (d, $J = 1.7$ Hz, 1H), 8.08–8.02 (m, 2H), 7.93 (dd, $J = 20.3$, 1.9 Hz, 1H), 7.82 (ddd, $J = 8.0$, 3.9, 1.8 Hz, 1H), 7.40 (d, $J = 8.0$ Hz, 1H), 7.18 (d, $J = 8.5$ Hz, 1H), 7.08 (dd, $J = 9.0$, 5.7 Hz, 1H), 4.79 (dd, $J = 14.1$, 8.7 Hz, 1H), 4.54–4.49 (m, 2H), 4.29 (td, $J = 8.9$, 8.2, 3.6 Hz, 1H), 3.90 (s, 1H), 3.65 (d, $J = 7.5$ Hz, 1H), 3.33 (s, 3H), 3.00 (t, $J = 1.3$ Hz, 3H), 2.80 (d, $J = 0.9$ Hz, 3H), 2.40 (s, 3H), 2.20 (s, 3H), 2.14 (d, $J = 13.7$ Hz, 1H), 1.97 (dt, $J = 13.7$, 7.2 Hz, 3H), 1.85 (d, $J = 6.5$ Hz, 3H), 1.36 (s, 3H), 1.29 (d, $J = 2.2$ Hz, 3H), 0.94 (dd, $J = 6.7$, 3.0 Hz, 6H), 0.81 (d, $J = 6.6$ Hz, 3H), 0.78–0.75 (m, 3H); ^{13}C NMR (101 MHz, DMSO) δ 173.92, 171.63, 171.13, 170.61, 153.71, 150.72, 141.54, 140.52, 135.16, 131.09, 127.32, 127.00, 126.73, 122.94, 60.20, 57.32, 56.54, 53.68, 47.74, 47.05, 37.18, 35.46, 30.81, 30.30, 29.45, 28.68, 25.91, 25.27, 24.99, 23.70, 19.95, 19.59, 18.26, 17.75; IR (Neat) 3239, 2957, 2924, 2854, 1688, 1658, 1600, 1577, 1534, 1508, 1494, 1465, 1412, 1321, 1296, 1231, 1188, 1145, 1120, 1033, 842, 785, 738, 698, 659, 558, 464, 411 cm⁻¹; HRMS (MM: ESI-APCI+) m/z calc'd for C₄₂H₅₈N₁₁O₆ [M + H]⁺: 812.4572; found: 812.4582.

4.1.27. (R)-N-(1-(((S)-1-(dimethylamino)-3-methyl-1-oxobutan-2-yl)amino)-2-methyl-1-oxopropan-2-yl)-1-((4-methyl-3-(1-methyl-7-((6-methylpyridin-3-yl)amino)-2-oxo-1,4-dihydropyrimido[4,5-d]pyrimidin-3(2H)-yl)benzoyl)-L-valyl)pyrrolidine-2-carboxamide (7o)

(Due to the distinct presence of rotameric isomers, the ^1H NMR and ^{13}C NMR contained extra peaks. See the attached spectrum in the supporting information) (Purity: 99%; HPLC); R_f : 0.35 (1:10 MeOH:CH₂Cl₂); $[\alpha]_D^{29} = +37.8$ (c 0.0530, MeOH); ^1H NMR (400 MHz, DMSO) δ 9.65 (s, 1H), 8.79 (d, $J = 2.6$ Hz, 1H), 8.48–8.41

(m, 1H), 8.15 (d, $J=1.7$ Hz, 1H), 8.07 (s, 1H), 8.05 (dd, $J=8.4, 2.7$ Hz, 1H), 7.93 (dd, $J=20.4, 1.8$ Hz, 1H), 7.82 (ddd, $J=8.0, 4.0, 1.8$ Hz, 1H), 7.40 (d, $J=8.0$ Hz, 1H), 7.18 (d, $J=8.5$ Hz, 1H), 7.09 (d, $J=9.0$ Hz, 1H), 4.79 (dd, $J=14.1, 8.8$ Hz, 1H), 4.50 (ddd, $J=19.3, 10.1, 5.6$ Hz, 3H), 4.31 (dd, $J=7.9, 4.7$ Hz, 1H), 3.94–3.83 (m, 1H), 3.68–3.55 (m, 1H), 3.33 (s, 3H), 3.00 (d, $J=1.4$ Hz, 3H), 2.80 (s, 3H), 2.40 (s, 3H), 2.20 (s, 3H), 2.17–2.08 (m, 1H), 1.98 (m, 3H), 1.87 (dd, $J=11.4, 5.7$ Hz, 2H), 1.36 (s, 3H), 1.29 (s, 3H), 0.94 (dd, $J=6.7, 2.9$ Hz, 6H), 0.79 (dd, $J=16.8, 6.7$ Hz, 6H); ^{13}C NMR (101 MHz, DMSO) δ 173.91, 171.63, 171.12, 159.41, 157.41, 150.71, 140.52, 139.70, 135.15, 131.08, 127.25, 126.99, 126.73, 122.93, 103.38, 100.20, 57.31, 56.54, 53.68, 47.73, 47.04, 37.17, 35.45, 30.81, 30.30, 29.44, 28.68, 25.90, 25.27, 24.99, 23.70, 19.95, 19.59, 18.25, 17.74; IR (Neat) 3296, 2957, 2871, 1627, 1606, 1575, 1525, 1492, 1410, 1332, 1290, 1233, 1195, 1140, 1112, 1071, 1034, 938, 831, 786, 731, 700, 621, 559, 516, 457, 408 cm^{-1} ; HRMS (MM: ESI-APCI+) m/z calc'd for $\text{C}_{42}\text{H}_{58}\text{N}_{11}\text{O}_6$ $[\text{M} + \text{H}]^+$: 812.4572; found: 812.4584.

4.1.28. *(S)-N-(1-(((S)-1-(dimethylamino)-4-methyl-1-oxopentan-2-yl)amino)-2-methyl-1-oxopropan-2-yl)-1-((4-methyl-3-(1-methyl-7-((6-methylpyridin-3-yl)amino)-2-oxo-1,4-dihydropyrimido[4,5-d]pyrimidin-3(2H)-yl)benzoyl)-L-isoleucyl)pyrrolidine-2-carboxamide (7p)*
(Due to the distinct presence of rotameric isomers, the ^1H NMR and ^{13}C NMR contained extra peaks. See the attached spectrum in the supporting information) (Purity: 96%; HPLC); R_f : 0.35 (1:10 MeOH:CH₂Cl₂); $[\alpha]_{\text{D}}^{28} = -54.7$ (c 0.0500, MeOH); ^1H NMR (600 MHz, DMSO) δ 9.64 (s, 1H), 8.79 (d, $J=2.6$ Hz, 1H), 8.46 (d, $J=8.1$ Hz, 1H), 8.15 (s, 1H), 8.05 (dd, $J=8.4, 2.6$ Hz, 1H), 8.00 (s, 1H), 7.92 (dd, $J=27.4, 1.9$ Hz, 1H), 7.82 (ddd, $J=8.2, 4.5, 1.9$ Hz, 1H), 7.40 (d, $J=8.1$ Hz, 1H), 7.25 (d, $J=8.6$ Hz, 1H), 7.18 (d, $J=8.5$ Hz, 1H), 4.78 (t, $J=13.6$ Hz, 1H), 4.72 (td, $J=8.6, 5.2$ Hz, 1H), 4.60–4.48 (m, 2H), 4.28 (dd, $J=7.8, 5.3$ Hz, 1H), 3.93 (d, $J=10.4$ Hz, 1H), 3.62 (d, $J=8.4$ Hz, 1H), 3.33 (s, 3H), 3.01–2.94 (m, 3H), 2.78 (s, 3H), 2.40 (s, 3H), 2.20 (s, 3H), 2.06–1.95 (m, 3H), 1.86 (d, $J=11.8$ Hz, 2H), 1.61–1.40 (m, 4H), 1.35 (s, 3H), 1.30 (s, 3H), 1.20–1.13 (m, 1H), 0.94 (d, $J=6.8$ Hz, 3H), 0.90–0.79 (m, 9H); ^{13}C NMR (151 MHz, DMSO) δ 173.61, 171.48, 171.30, 170.67, 170.62, 165.80, 165.67, 159.30, 157.30, 153.60, 152.55, 152.47, 150.60, 141.45, 141.42, 140.40, 139.64, 139.62, 135.05, 133.13, 133.05, 130.98, 127.22, 126.91, 126.61, 122.83, 103.27, 60.26, 60.24, 56.33, 55.72, 47.72, 47.04, 46.93, 41.24, 36.78, 36.01, 35.98, 35.50, 29.27, 28.58, 25.84, 25.82, 25.07, 24.96, 24.93, 24.91, 24.46, 23.60, 23.36, 22.33, 17.66, 17.63, 15.29, 10.91; IR (Neat) 3300, 2959, 2360, 2340, 1629, 1609, 1531, 1496, 1414, 1332, 1290, 1240, 1143, 1115, 845, 737 cm^{-1} ; HRMS (MM: ESI-APCI+) m/z calc'd for $\text{C}_{44}\text{H}_{62}\text{N}_{11}\text{O}_6$ $[\text{M} + \text{H}]^+$: 840.4885; found: 840.4885.

4.1.29. *(S)-N-(1-(((S)-1-(dimethylamino)-4-methyl-1-oxopentan-2-yl)amino)-2-methyl-1-oxopropan-2-yl)-1-((4-methyl-3-(1-methyl-7-((6-methylpyridin-3-yl)amino)-2-oxo-1,4-dihydropyrimido[4,5-d]pyrimidin-3(2H)-yl)benzoyl)-L-leucyl)pyrrolidine-2-carboxamide (7q)*
(Due to the distinct presence of rotameric isomers, the ^1H NMR and ^{13}C NMR contained extra peaks. See the attached spectrum in the supporting information) (Purity: 95%; HPLC); R_f : 0.35 (1:10 MeOH:CH₂Cl₂); $[\alpha]_{\text{D}}^{26} = -34.0$ (c 0.171, MeOH); ^1H NMR (400 MHz, DMSO) δ 9.63 (s, 1H), 8.78 (d, $J=2.6$ Hz, 1H), 8.38 (dd, $J=8.2, 2.3$ Hz, 1H), 8.14 (s, 1H), 8.07–8.00 (m, 2H), 7.91 (dd, $J=27.5, 1.9$ Hz, 1H), 7.84 (dd, $J=8.0, 1.9$ Hz, 1H), 7.41 (dd, $J=8.7, 2.6$ Hz, 2H), 7.18 (d, $J=8.5$ Hz, 1H), 4.84–4.63 (m, 3H), 4.51 (dd, $J=14.2, 5.3$ Hz, 1H), 4.26 (dd, $J=7.6, 4.9$ Hz, 1H), 3.73 (q, $J=6.5$ Hz, 1H), 3.55 (dd, $J=15.4, 6.4$ Hz, 2H), 3.33 (d, $J=2.0$ Hz, 3H), 2.95 (d,

$J=2.1$ Hz, 3H), 2.77 (s, 3H), 2.40 (s, 3H), 2.20 (s, 3H), 2.06–1.94 (m, 2H), 1.87 (td, $J=10.4, 5.7$ Hz, 2H), 1.73 (t, $J=11.4$ Hz, 2H), 1.51 (tt, $J=17.5, 9.3$ Hz, 2H), 1.40 (d, $J=8.9$ Hz, 1H), 1.36 (s, 3H), 1.30 (s, 3H), 0.96–0.89 (m, 6H), 0.85 (dd, $J=9.8, 6.5$ Hz, 6H); ^{13}C NMR (101 MHz, DMSO) δ 173.79, 171.50, 171.47, 171.26, 159.40, 157.40, 150.74, 140.49, 139.82, 135.14, 131.16, 126.79, 122.98, 103.38, 60.49, 56.50, 49.92, 47.30, 47.04, 41.39, 36.81, 35.63, 29.12, 28.68, 26.01, 25.18, 24.99, 24.85, 24.49, 23.76, 23.66, 23.49, 22.43, 21.68, 21.65, 17.74. IR (Neat) 3298, 2924, 1628, 1605, 1576, 1528, 1493, 1448, 1411, 1332, 1288, 1264, 1235, 1194, 1142, 1112, 1075, 1031, 943, 830, 787, 732, 700, 623, 548, 514, 480, 458 cm^{-1} ; HRMS (MM: ESI-APCI+) m/z calc'd for $\text{C}_{44}\text{H}_{62}\text{N}_{11}\text{O}_6$ $[\text{M} + \text{H}]^+$: 840.4806; found: 840.4885.

4.1.30. *(S)-N-(1-(((S)-1-(dimethylamino)-4-methyl-1-oxopentan-2-yl)amino)-2-methyl-1-oxopropan-2-yl)-1-((4-methyl-3-(1-methyl-7-((6-methylpyridin-3-yl)amino)-2-oxo-1,4-dihydropyrimido[4,5-d]pyrimidin-3(2H)-yl)benzoyl)glycyl)pyrrolidine-2-carboxamide (7r)*

(Due to the distinct presence of rotameric isomers, the ^1H NMR and ^{13}C NMR contained extra peaks. See the attached spectrum in the supporting information) (Purity: 97%; HPLC); R_f : 0.35 (1:10 MeOH:CH₂Cl₂); $[\alpha]_{\text{D}}^{30} = -27.0$ (c 0.100, MeOH); ^1H NMR (600 MHz, DMSO) δ 9.64 (d, $J=2.4$ Hz, 1H), 8.79 (d, $J=2.7$ Hz, 1H), 8.17–8.09 (m, 2H), 8.05 (d, $J=8.6, 2.5$ Hz, 1H), 7.96 (d, $J=22.1, 1.8$ Hz, 1H), 7.86 (dd, $J=13.2, 5.9$ Hz, 1H), 7.42 (d, $J=8.0$ Hz, 1H), 7.33 (dd, $J=18.9, 8.8$ Hz, 1H), 7.17 (d, $J=8.4$ Hz, 1H), 4.80–4.71 (m, 1H), 4.68 (m, $J=8.9, 5.2$ Hz, 1H), 4.52 (d, $J=14.0, 4.2$ Hz, 1H), 4.29 (m, $J=5.8, 5.2$ Hz, 1H), 3.97 (m, $J=21.2, 17.0, 4.6$ Hz, 1H), 3.58 (m, $J=6.2$ Hz, 1H), 3.32 (s, 3H), 3.00–2.91 (m, 3H), 2.79 (d, 3H), 2.40 (s, 3H), 2.21 (s, 3H), 2.11–1.95 (m, 2H), 1.93–1.74 (m, 2H), 1.50 (qd, $J=13.7, 6.5$ Hz, 1H), 1.39 (m, 2H), 1.34 (s, 3H), 1.29 (s, 3H), 0.79 (m, 6H). ^{13}C NMR (151 MHz, DMSO) δ 173.59, 173.45, 171.68, 171.45, 171.44, 171.41, 171.20, 167.88, 167.51, 167.48, 165.76, 165.66, 159.30, 157.34, 157.31, 153.58, 152.50, 152.48, 152.46, 150.59, 141.58, 141.56, 141.53, 140.41, 140.39, 139.74, 139.72, 139.60, 139.58, 135.05, 133.30, 133.15, 133.12, 131.10, 131.07, 126.95, 126.89, 126.82, 126.70, 126.61, 126.59, 122.82, 103.29, 60.23, 59.40, 56.44, 56.40, 47.15, 46.99, 46.98, 46.94, 46.50, 42.40, 41.88, 41.32, 36.81, 36.65, 36.62, 35.49, 35.40, 35.37, 32.05, 29.02, 28.99, 28.59, 28.57, 28.55, 26.33, 26.27, 25.65, 24.88, 24.85, 24.84, 24.59, 24.42, 24.08, 24.05, 23.59, 23.49, 23.42, 23.36, 22.33, 22.20, 22.18, 22.07, 22.05, 17.64; IR (Neat) 3402, 2926, 1610, 1533, 1499, 1463, 1417, 1276, 1120, 846, 750 cm^{-1} ; HRMS (MM: ESI-APCI+) m/z calc'd for $\text{C}_{40}\text{H}_{54}\text{N}_{11}\text{O}_6$ $[\text{M} + \text{H}]^+$: 784.4259; found: 784.4257.

4.1.31. *(S)-1-(((S)-2-cyclohexyl-2-(4-methyl-3-(1-methyl-7-((6-methylpyridin-3-yl)amino)-2-oxo-1,4-dihydropyrimido[4,5-d]pyrimidin-3(2H)-yl)benzamido)acetyl)-N-(1-(((S)-1-(dimethylamino)-4-methyl-1-oxopentan-2-yl)amino)-2-methyl-1-oxopropan-2-yl)pyrrolidine-2-carboxamide (7s)*

(Due to the distinct presence of rotameric isomers, the ^1H NMR and ^{13}C NMR contained extra peaks. See the attached spectrum in the supporting information) (Purity: 97%; HPLC); R_f : 0.35 (1:10 MeOH:CH₂Cl₂); $[\alpha]_{\text{D}}^{29} = -51.4$ (c 0.0390, MeOH); ^1H NMR (400 MHz, DMSO) δ 9.66 (s, 1H), 8.81 (d, $J=2.6$ Hz, 1H), 8.38 (d, $J=8.3$ Hz, 1H), 8.16 (s, 1H), 8.07 (dd, $J=8.5, 2.7$ Hz, 1H), 7.94 (dd, $J=17.8, 1.8$ Hz, 2H), 7.84 (d, $J=8.0$ Hz, 1H), 7.45–7.37 (m, 2H), 7.19 (d, $J=8.5$ Hz, 1H), 4.80 (dd, $J=14.0, 7.5$ Hz, 1H), 4.77–4.65 (m, 1H), 4.63–4.48 (m, 2H), 4.29 (t, $J=6.2$ Hz, 1H), 3.90 (s, 1H), 3.64 (s, 1H), 3.35 (s, 3H), 3.00 (s, 3H), 2.80 (s, 3H), 2.42 (s, 3H), 2.22 (s, 3H), 2.14–1.77 (m, 8H), 1.65 (d, $J=19.5$ Hz, 2H), 1.57 (m, 1H),

1.50–1.32 (m, 8H), 1.21 (d, $J=32.8$ Hz, 3H), 1.05 (d, $J=15.2$ Hz, 2H), 0.92–0.86 (m, 6H); ^{13}C NMR (101 MHz, DMSO) δ 177.65, 173.79, 171.55, 171.21, 170.71, 169.57, 159.41, 153.76, 150.71, 141.57, 140.51, 139.73, 138.69, 135.16, 131.10, 127.38, 126.97, 126.72, 122.94, 117.93, 103.38, 84.38, 56.45, 47.79, 47.25, 41.35, 36.87, 35.62, 29.13, 28.68, 25.51, 25.28, 25.06, 24.64, 23.70, 22.46, 17.76; IR (Neat) 3300, 2927, 2854, 2360, 2340, 1629, 1609, 1530, 1496, 1414, 1334, 1289, 1236, 1192, 1143, 1117, 845, 788, 737 cm^{-1} ; HRMS (MM: ESI-APCI+) m/z calc'd for $\text{C}_{46}\text{H}_{64}\text{N}_{11}\text{O}_6$ $[\text{M} + \text{H}]^+$: 866.5041; found: 866.5021.

4.1.32. (S)-N-1-(((S)-1-(dimethylamino)-4-methyl-1-oxopentan-2-yl)amino)-2-methyl-1-oxopropan-2-yl)-1-((S)-2-(4-methyl-3-(1-methyl-7-((6-methylpyridin-3-yl)amino)-2-oxo-1,4-dihydropyrimido[4,5-d]pyrimidin-3(2H)-yl)benzamido)pentanoyl)pyrrolidine-2-carboxamide (7t)

(Due to the distinct presence of rotameric isomers, the ^1H NMR and ^{13}C NMR contained extra peaks. See the attached spectrum in the supporting information) (Purity: 99%; HPLC); R_f : 0.35 (1:10 MeOH: CH_2Cl_2); $[\alpha]_{\text{D}}^{20} = +24.8$ (c 0.0556, MeOH); ^1H NMR (400 MHz, DMSO) δ 9.65 (s, 1H), 8.80 (d, $J=2.6$ Hz, 1H), 8.41–8.34 (m, 1H), 8.15 (s, 1H), 8.08–7.99 (m, 2H), 7.98–7.89 (m, 1H), 7.87–7.82 (m, 1H), 7.41 (t, $J=7.2$ Hz, 2H), 7.18 (d, $J=8.5$ Hz, 1H), 4.83–4.66 (m, 3H), 4.53 (dd, $J=14.0$, 5.1 Hz, 1H), 4.27 (t, $J=6.2$ Hz, 1H), 3.75 (d, $J=7.8$ Hz, 1H), 3.58 (s, 1H), 3.33 (s, 3H), 2.97 (d, $J=2.4$ Hz, 3H), 2.79 (s, 3H), 2.41 (s, 3H), 2.21 (s, 3H), 1.99 (dd, $J=14.4$, 7.9 Hz, 2H), 1.88 (s, 2H), 1.76–1.69 (m, 2H), 1.53 (dt, $J=15.1$, 7.7 Hz, 2H), 1.42 (d, $J=18.8$ Hz, 3H), 1.37 (s, 3H), 1.31 (s, 3H), 0.92 (d, $J=7.2$ Hz, 3H), 0.85 (dd, $J=9.6$, 6.4 Hz, 6H); ^{13}C NMR (101 MHz, DMSO) δ 173.76, 171.48, 171.02, 165.80, 165.68, 159.41, 157.42, 152.61, 150.72, 141.62, 140.52, 139.79, 135.16, 131.15, 126.73, 122.94, 103.38, 60.50, 56.50, 51.45, 47.41, 47.26, 47.06, 41.39, 36.82, 35.59, 33.53, 29.15, 28.68, 26.04, 25.18, 25.04, 24.50, 23.71, 23.49, 22.45, 19.21, 17.76, 14.21; IR (Neat) 3288, 2955, 2918, 2849, 1727, 1633, 1607, 1577, 1532, 1497, 1462, 1411, 1378, 1294, 1118, 1099, 1019, 800, 739 cm^{-1} ; HRMS (MM: ESI-APCI+) m/z calc'd for $\text{C}_{43}\text{H}_{59}\text{N}_{11}\text{O}_6\text{Na}$ $[\text{M} + \text{Na}]^+$: 848.4547; found: 848.4550.

4.1.33. (S)-N-1-((2-(dimethylamino)-2-oxoethyl)amino)-2-methyl-1-oxopropan-2-yl)-1-((4-methyl-3-(1-methyl-7-((6-methylpyridin-3-yl)amino)-2-oxo-1,4-dihydropyrimido[4,5-d]pyrimidin-3(2H)-yl)benzoyl)-L-valyl)pyrrolidine-2-carboxamide (7u)

(Due to the distinct presence of rotameric isomers, the ^1H NMR and ^{13}C NMR contained extra peaks. See the attached spectrum in the supporting information) (Purity: 96%; HPLC); R_f : 0.35 (1:10 MeOH: CH_2Cl_2); $[\alpha]_{\text{D}}^{27} = -59.5$ (c 0.0240, MeOH); ^1H NMR (600 MHz, DMSO) δ 9.65 (s, 1H), 8.79 (d, $J=2.6$ Hz, 1H), 8.49 (dd, $J=8.2$, 4.1 Hz, 1H), 8.26 (s, 1H), 8.15 (d, $J=3.7$ Hz, 1H), 8.05 (dd, $J=8.4$, 2.7 Hz, 1H), 7.93 (dd, $J=29.6$, 1.9 Hz, 1H), 7.82 (ddd, $J=7.8$, 5.8, 1.9 Hz, 1H), 7.47 (t, $J=5.3$ Hz, 1H), 7.40 (dd, $J=8.2$, 1.9 Hz, 1H), 7.18 (d, $J=8.5$ Hz, 1H), 4.78 (dd, $J=16.0$, 14.1 Hz, 1H), 4.53–4.45 (m, 2H), 4.30 (t, $J=6.8$ Hz, 1H), 4.00 (dd, $J=16.6$, 5.8 Hz, 1H), 3.96 (q, $J=7.7$ Hz, 1H), 3.61 (ddd, $J=16.8$, 12.0, 6.1 Hz, 2H), 3.33 (s, 3H), 2.93 (s, 3H), 2.80 (s, 3H), 2.40 (s, 3H), 2.20 (d, $J=1.5$ Hz, 3H), 2.14 (dd, $J=13.5$, 6.4 Hz, 1H), 2.08–1.97 (m, 2H), 1.86 (qd, $J=12.1$, 11.4, 5.3 Hz, 2H), 1.34 (d, $J=12.4$ Hz, 6H), 0.97–0.92 (m, 6H); ^{13}C NMR (151 MHz, DMSO) δ 174.17, 171.68, 170.83, 170.79, 168.40, 165.92, 165.77, 159.30, 157.30, 153.60, 152.55, 152.48, 150.60, 141.45, 141.42, 140.40, 139.63, 135.04, 133.13, 133.04, 131.00, 127.21, 127.15, 126.91, 126.61, 122.83, 103.28, 63.15, 60.24, 60.21, 57.21, 56.39, 47.80, 46.93, 35.98, 35.38, 30.42, 30.37, 29.12, 28.58,

25.96, 25.94, 25.16, 25.13, 25.12, 23.60, 19.40, 19.38, 19.17, 17.66, 17.63; IR (Neat) 3289, 2927, 1605, 1575, 1528, 1493, 1411, 1332, 1289, 1234, 1195, 1142, 1113, 1033, 947, 842, 786, 731 cm^{-1} ; HRMS (MM: ESI-APCI+) m/z calc'd for $\text{C}_{39}\text{H}_{52}\text{N}_{11}\text{O}_6$ $[\text{M} + \text{H}]^+$: 770.4102; found: 770.4101.

4.1.34. (R)-N-((S)-3-methyl-1-oxo-1-(((R)-1-phenylethyl)amino)butan-2-yl)-1-((4-methyl-3-(1-methyl-7-((6-methylpyridin-3-yl)amino)-2-oxo-1,4-dihydropyrimido[4,5-d]pyrimidin-3(2H)-yl)benzoyl)-L-valyl)pyrrolidine-2-carboxamide (7v)

(Due to the distinct presence of rotameric isomers, the ^1H NMR and ^{13}C NMR contained extra peaks. See the attached spectrum in the supporting information) (Purity: 95%; HPLC); R_f : 0.35 (1:10 MeOH: CH_2Cl_2); $[\alpha]_{\text{D}}^{29} = +4.25$ (c 0.230, MeOH); ^1H NMR (400 MHz, DMSO) δ 10.60 (s, 1H), 8.93–8.89 (m, 1H), 8.84 (s, 1H), 8.53 (dd, $J=7.3$, 3.1 Hz, 1H), 8.20 (d, $J=8.0$ Hz, 1H), 8.07 (dd, $J=8.4$, 2.7 Hz, 1H), 7.94–7.87 (m, 1H), 7.83 (s, 1H), 7.45 (d, $J=8.0$ Hz, 1H), 7.40–7.32 (m, 2H), 7.31–7.24 (m, 5H), 4.92–4.79 (m, 1H), 4.45–4.34 (m, 2H), 4.09–3.99 (m, 1H), 3.96 (s, 1H), 3.66–3.58 (m, 1H), 3.53 (d, $J=4.0$ Hz, 3H), 3.46–3.37 (m, 1H), 3.67–3.56 (m, 1H), 2.45 (s, 3H), 2.13 (s, 3H), 2.08–1.98 (m, 2H), 1.97–1.75 (m, 5H), 1.27 (d, $J=7.0$ Hz, 3H), 0.98 (d, $J=6.6$ Hz, 6H), 0.76 (t, $J=6.6$ Hz, 3H), 0.62 (dd, $J=6.9$, 4.3 Hz, 3H); ^{13}C NMR (101 MHz, DMSO) δ 172.56, 171.70, 170.91, 170.32, 170.23, 166.19, 165.84, 161.86, 160.08, 159.76, 159.68, 158.24, 152.92, 151.03, 150.97, 144.74, 144.63, 141.79, 140.38, 134.97, 133.63, 132.87, 132.75, 130.85, 130.71, 129.02, 128.58, 128.50, 128.40, 127.02, 126.94, 126.62, 126.46, 123.20, 101.11, 60.34, 59.75, 58.39, 57.91, 57.12, 48.21, 48.05, 47.67, 47.12, 32.92, 31.30, 30.37, 30.14, 29.87, 29.57, 29.42, 24.48, 23.86, 22.77, 22.73, 22.42, 19.79, 19.66, 19.58, 19.47, 19.41, 18.84, 18.49, 17.45; IR (Neat) 3294, 2956, 2922, 2853, 1725, 1664, 1595, 1571, 1529, 1494, 1462, 1398, 1377, 1333, 1300, 1267, 1236, 1207, 1174, 1115, 1070, 1030, 958, 916, 885, 829, 804, 756, 732, 699, 670, 629, 596, 560, 501, 460, 447, 426 cm^{-1} ; HRMS (MM: ESI-APCI+) m/z calc'd for $\text{C}_{44}\text{H}_{55}\text{N}_{10}\text{O}_5$ $[\text{M} + \text{H}]^+$: 803.4357; found: 803.4371.

4.1.35. (R)-N-((S)-3-methyl-1-oxo-1-(((R)-1-phenylethyl)amino)butan-2-yl)-1-((4-methyl-3-(1-methyl-7-((6-methylpyridin-3-yl)amino)-2-oxo-1,4-dihydropyrimido[4,5-d]pyrimidin-3(2H)-yl)benzoyl)-L-phenylalanyl)pyrrolidine-2-carboxamide (7w)

(Due to the distinct presence of rotameric isomers, the ^1H NMR and ^{13}C NMR contained extra peaks. See the attached spectrum) (Purity: 99%; HPLC); R_f : 0.35 (1:10 MeOH: CH_2Cl_2); $[\alpha]_{\text{D}}^{27} = +104$ (c 0.0560, MeOH); (Due to the distinct presence of rotameric isomers, the ^1H NMR and ^{13}C NMR contained extra peaks. See the attached spectrum in the supporting information) ^1H NMR (400 MHz, DMSO) δ 9.66 (d, $J=3.8$ Hz, 1H), 8.83 (t, $J=5.6$ Hz, 1H), 8.80–8.75 (m, 1H), 8.21–8.10 (m, 2H), 8.05 (dt, $J=8.4$, 2.2 Hz, 1H), 7.89 (dd, $J=3.7$, 1.8 Hz, 1H), 7.80–7.73 (m, 1H), 7.49–7.32 (m, 2H), 7.32–7.26 (m, 5H), 7.25–7.09 (m, 5H), 6.98–6.89 (m, 1H), 4.91–4.83 (m, 1H), 4.80 (dd, $J=8.9$, 6.9 Hz, 1H), 4.67 (d, $J=14.0$ Hz, 1H), 4.55–4.50 (m, 1H), 4.34–4.21 (m, 1H), 3.69 (s, 1H), 3.17 (d, $J=5.2$ Hz, 1H), 3.06 (d, $J=7.6$ Hz, 1H), 3.02–2.84 (m, 1H), 2.41 (s, 3H), 2.19 (d, $J=14.1$ Hz, 3H), 2.08 (s, 3H), 2.06–1.92 (m, 1H), 1.84–1.65 (m, 3H), 1.29–1.21 (m, 3H), 0.92–0.64 (m, 6H); ^{13}C NMR (101 MHz, DMSO) δ 171.65, 171.62, 170.78, 170.73, 170.30, 170.27, 170.14, 165.98, 165.82, 159.45, 157.42, 153.73, 152.53, 152.51, 150.73, 144.80, 144.76, 141.53, 140.54, 139.93, 139.79, 138.78, 137.81, 137.77, 135.15, 132.83, 132.78, 131.01, 129.77, 129.59, 128.66, 128.58, 128.34, 127.13, 126.99, 126.81,

126.78, 126.74, 126.42, 122.93, 103.29, 60.34, 58.51, 58.42, 53.96, 53.85, 53.62, 49.07, 48.46, 48.17, 47.16, 47.04, 31.15, 30.26, 29.78, 28.68, 23.70, 22.75, 22.70, 19.73, 19.60, 19.46, 18.54, 18.47, 18.14, 17.76; IR (Neat) 3291, 2966, 1640, 1607, 1574, 1531, 1496, 1451, 1414, 1332, 1292, 1235, 1193, 1145, 1118, 1029, 843, 739, 701 cm^{-1} ; HRMS (MM: ESI-APCI+) m/z calc'd for $\text{C}_{48}\text{H}_{55}\text{N}_{10}\text{O}_5$ $[\text{M} + \text{H}]^+$: 851.4357; found: 851.4377.

4.1.36. (R)-3-benzyl-N-(4-methyl-3-(1-methyl-7-((6-methylpyridin-3-yl)amino)-2-oxo-1,4-dihydropyrimido[4,5-d]pyrimidin-3(2H)-yl)phenyl)-2-oxo-5-phenyl-2,3-dihydro-1H-benzo[e][1,4]diazepine-8-carboxamide (11f)

(Purity: 96%; HPLC); R_f : 0.35 (1:10 MeOH: CH_2Cl_2); $[\alpha]_{\text{D}}^{21} = -62.7$ (c 0.0390, MeOH); ^1H NMR (400 MHz, DMSO) δ 10.85 (s, 1H), 10.57 (s, 1H), 9.65 (s, 1H), 8.80 (d, $J = 2.6$ Hz, 1H), 8.16 (d, $J = 1.7$ Hz, 1H), 8.05 (dd, $J = 8.4, 2.7$ Hz, 1H), 7.85 (dd, $J = 4.2, 2.2$ Hz, 1H), 7.79 (d, $J = 1.7$ Hz, 1H), 7.72 (dd, $J = 8.2, 1.7$ Hz, 1H), 7.62 (dd, $J = 8.3, 2.2$ Hz, 1H), 7.53–7.48 (m, 1H), 7.46–7.42 (m, 4H), 7.37–7.33 (m, 3H), 7.28 (td, $J = 8.1, 6.2$ Hz, 3H), 7.18 (dd, $J = 8.0, 5.3$ Hz, 2H), 4.71 (d, $J = 14.0$ Hz, 1H), 4.52 (d, $J = 14.1$ Hz, 1H), 3.73 (dd, $J = 8.1, 5.4$ Hz, 1H), 3.47–3.35 (m, 2H), 2.40 (s, 3H), 2.13 (s, 3H); ^{13}C NMR (101 MHz, DMSO) δ 170.54, 167.78, 159.42, 157.48, 152.55, 150.67, 141.62, 140.52, 139.76, 139.66, 139.01, 138.18, 135.18, 131.30, 131.14, 130.91, 130.18, 129.76, 129.12, 128.80, 128.54, 126.72, 126.49, 122.92, 121.27, 47.12, 40.63, 40.43, 40.22, 40.01, 39.80, 39.59, 39.38, 28.70, 23.70, 17.27; IR (Neat) 3298, 2925, 1671, 1601, 1535, 1413, 1321, 1119, 1032, 747, 698 cm^{-1} ; HRMS (MM: ESI-APCI+) m/z calc'd for $\text{C}_{43}\text{H}_{37}\text{N}_9\text{O}_3\text{Na}$ $[\text{M} + \text{Na}]^+$: 750.2917; found: 750.2933.

4.1.37. (S)-3-(4-fluorobenzyl)-N-(4-methyl-3-(1-methyl-7-((6-methylpyridin-3-yl)amino)-2-oxo-1,4-dihydropyrimido[4,5-d]pyrimidin-3(2H)-yl)phenyl)-2-oxo-5-phenyl-2,3-dihydro-1H-benzo[e][1,4]diazepine-8-carboxamide (11g)

(Purity: 95%; HPLC); R_f : 0.35 (1:10 MeOH: CH_2Cl_2); $[\alpha]_{\text{D}}^{30} = +0.706$ (c 0.0940, MeOH); ^1H NMR (600 MHz, DMSO) δ 10.83 (s, 1H), 10.51 (s, 1H), 9.64 (s, 1H), 8.80 (s, 1H), 8.16 (s, 1H), 8.05 (d, $J = 7.2$ Hz, 1H), 7.84 (d, $J = 5.8$ Hz, 1H), 7.76 (s, 1H), 7.70 (d, $J = 8.3$ Hz, 1H), 7.60 (d, $J = 8.3$ Hz, 1H), 7.51 (m, 2H), 7.47–7.35 (m, 8H), 7.30 (d, $J = 8.4$ Hz, 1H), 7.18 (d, $J = 8.4$ Hz, 1H), 7.10 (t, $J = 8.7$ Hz, 3H), 4.71 (d, $J = 14.0$ Hz, 1H), 4.53 (d, $J = 14.0$ Hz, 1H), 3.73 (t, $J = 6.8$ Hz, 1H), 3.41 (dd, $J = 13.2, 5.3$ Hz, 2H), 2.40 (s, 3H), 2.13 (s, 3H); ^{13}C NMR (151 MHz, DMSO) δ 170.10, 167.41, 164.40, 161.62, 160.02, 158.94, 157.01, 153.26, 152.09, 150.22, 141.17, 140.03, 139.28, 138.53, 137.73, 135.25 (d, $J = 2.9$ Hz), 134.71, 131.51 (d, $J = 7.6$ Hz), 130.87, 130.77, 130.75, 129.57 (d, $J = 271.9$ Hz), 129.30, 129.25, 128.35, 126.23, 122.47, 121.37, 120.76, 119.62, 119.06, 119.03, 114.72 (d, $J = 20.9$ Hz), 102.95, 65.00, 46.64, 38.25, 36.26, 28.24, 23.24, 16.81; ^{19}F NMR (377 MHz, DMSO) δ -117.19; IR (Neat) 3324, 2925, 2854, 1674, 1607, 1511, 1463, 1408, 1261, 1100, 748, 669 cm^{-1} ; HRMS (MM: ESI-APCI+) m/z calc'd for $\text{C}_{43}\text{H}_{37}\text{FN}_9\text{O}_3$ $[\text{M} + \text{H}]^+$: 746.3003; found: 746.3005.

4.1.38. (S)-3-isobutyl-1-methyl-N-(4-methyl-3-(1-methyl-7-((6-methylpyridin-3-yl)amino)-2-oxo-1,4-dihydropyrimido[4,5-d]pyrimidin-3(2H)-yl)phenyl)-2-oxo-5-phenyl-2,3-dihydro-1H-benzo[e][1,4]diazepine-8-carboxamide (11h)

(Purity: 99%; HPLC); R_f : 0.35 (1:10 MeOH: CH_2Cl_2); $[\alpha]_{\text{D}}^{26} = +55.8$ (c 0.110, MeOH); ^1H NMR (600 MHz, DMSO) δ 10.53 (s, 1H), 9.76 (s, 1H), 8.87 (t, $J = 2.5$ Hz, 1H), 8.18 (s, 1H), 8.12 (d, $J = 8.5$ Hz, 1H),

8.06 (s, 1H), 7.85–7.81 (m, 1H), 7.80 (d, $J = 8.2$ Hz, 1H), 7.65–7.61 (m, 1H), 7.55 (d, $J = 7.6$ Hz, 2H), 7.52 (d, $J = 7.3$ Hz, 1H), 7.46 (dd, $J = 11.7, 7.8$ Hz, 3H), 7.33 (d, $J = 8.4$ Hz, 1H), 7.27 (d, $J = 8.5$ Hz, 1H), 4.72 (d, $J = 14.0$ Hz, 1H), 4.55 (d, $J = 14.0$ Hz, 1H), 3.62 (ddq, $J = 9.6, 6.8, 3.4, 2.8$ Hz, 1H), 3.57 (dt, $J = 8.9, 5.4$ Hz, 1H), 3.35 (s, 3H), 3.14 (qd, $J = 7.4, 4.1$ Hz, 2H), 2.44 (s, 3H), 2.15 (s, 4H), 1.92–1.78 (m, 2H), 0.94 (d, $J = 6.4$ Hz, 3H), 0.76 (d, $J = 6.3$ Hz, 3H); ^{13}C NMR (151 MHz, DMSO) δ 170.28, 167.36, 164.71, 159.15, 157.42, 153.61, 152.45, 149.85, 143.69, 141.53, 138.36, 138.03, 137.98, 135.53, 131.31, 131.17, 130.91, 130.80, 130.16, 129.57, 128.76, 123.56, 123.31, 121.38, 120.16, 119.61, 103.59, 61.52, 53.96, 46.99, 42.21, 35.10, 28.64, 24.53, 23.74, 22.93, 22.14, 18.45, 17.17, 17.09, 12.86; IR (Neat) 2954, 2360, 2340, 1659, 1599, 1533, 1492, 1411, 1323, 1266, 1188, 1143, 1030, 837, 784, 733, 698 cm^{-1} ; HRMS (MM: ESI-APCI+) m/z calc'd for $\text{C}_{41}\text{H}_{42}\text{N}_9\text{O}_3$ $[\text{M} + \text{H}]^+$: 708.3411; found: 708.3407.

4.1.39. (S)-1-allyl-3-isobutyl-N-(4-methyl-3-(1-methyl-7-((6-methylpyridin-3-yl)amino)-2-oxo-1,4-dihydropyrimido[4,5-d]pyrimidin-3(2H)-yl)phenyl)-2-oxo-5-phenyl-2,3-dihydro-1H-benzo[e][1,4]diazepine-8-carboxamide (11i)

(Purity: 96%; HPLC); R_f : 0.35 (1:10 MeOH: CH_2Cl_2); $[\alpha]_{\text{D}}^{28} = +44.6$ (c 0.180, MeOH); ^1H NMR (600 MHz, DMSO) δ 10.51 (s, 1H), 9.65 (s, 1H), 8.89–8.64 (m, 1H), 8.14 (d, $J = 31.3$ Hz, 2H), 8.08–8.01 (m, 1H), 7.81 (m, 2H), 7.62 (d, $J = 8.3$ Hz, 1H), 7.57–7.39 (m, 6H), 7.32 (d, $J = 8.3$ Hz, 1H), 7.18 (d, $J = 8.3$ Hz, 1H), 5.76 (ddt, $J = 16.1, 10.3, 5.0$ Hz, 1H), 5.04 (d, $J = 10.4$ Hz, 1H), 4.98 (d, $J = 17.3$ Hz, 1H), 4.73 (dd, $J = 18.1, 7.8$ Hz, 2H), 4.60–4.50 (m, 2H), 3.64 (dd, $J = 8.8, 4.5$ Hz, 1H), 3.34 (s, 3H), 2.40 (s, 3H), 2.14 (s, 3H), 2.11 (m, 1H), 1.88 (dd, $J = 12.9, 7.1$ Hz, 2H), 0.94 (d, $J = 5.7$ Hz, 3H), 0.77 (d, $J = 5.6$ Hz, 3H); ^{13}C NMR (151 MHz, DMSO) δ 169.22, 167.53, 164.63, 159.31, 157.38, 153.62, 152.48, 150.58, 142.44, 141.56, 140.39, 138.37, 138.02, 138.00, 135.06, 133.77, 131.85, 131.33, 131.16, 130.93, 130.15, 129.45, 128.84, 126.59, 123.70, 122.83, 122.08, 120.15, 120.13, 119.63, 119.60, 116.64, 103.31, 61.69, 49.16, 47.00, 40.42, 28.61, 24.63, 23.66, 23.60, 22.30, 17.17; IR (Neat) 3294, 2953, 2360, 2340, 1663, 1598, 1532, 1491, 1410, 1293, 1231, 1187, 1142, 1119, 1030, 989, 914, 841, 784, 739, 697 cm^{-1} ; HRMS (MM: ESI-APCI+) m/z calc'd for $\text{C}_{43}\text{H}_{44}\text{N}_9\text{O}_3$ $[\text{M} + \text{H}]^+$: 734.3567; found: 734.3565.

4.1.40. (S)-1,3-diisobutyl-N-(4-methyl-3-(1-methyl-7-((6-methylpyridin-3-yl)amino)-2-oxo-1,4-dihydropyrimido[4,5-d]pyrimidin-3(2H)-yl)phenyl)-2-oxo-5-phenyl-2,3-dihydro-1H-benzo[e][1,4]diazepine-8-carboxamide (11j)

(Purity: 97%; HPLC); R_f : 0.35 (1:10 MeOH: CH_2Cl_2); $[\alpha]_{\text{D}}^{31} = +21.4$ (c 0.0889, MeOH); ^1H NMR (600 MHz, DMSO) δ 10.48 (s, 1H), 9.65 (s, 1H), 8.80 (d, $J = 2.6$ Hz, 1H), 8.17 (d, $J = 3.0$ Hz, 2H), 8.05 (dd, $J = 8.6, 2.7$ Hz, 1H), 7.86–7.77 (m, 2H), 7.64 (dt, $J = 5.9, 2.9$ Hz, 1H), 7.57–7.51 (m, 3H), 7.48 (t, $J = 7.4$ Hz, 2H), 7.44 (d, $J = 8.1$ Hz, 1H), 7.33 (d, $J = 8.4$ Hz, 1H), 7.18 (d, $J = 8.5$ Hz, 1H), 4.71 (d, $J = 13.9$ Hz, 1H), 4.54 (d, $J = 14.0$ Hz, 1H), 4.21 (dd, $J = 13.8, 8.9$ Hz, 1H), 3.66 (dd, $J = 13.8, 5.9$ Hz, 1H), 3.57 (dd, $J = 8.9, 4.4$ Hz, 1H), 3.34 (s, 3H), 2.41 (s, 3H), 2.15 (s, 3H), 2.14–2.09 (m, 1H), 1.83 (tt, $J = 13.0, 7.4$ Hz, 2H), 1.66 (p, $J = 6.7$ Hz, 1H), 0.93 (d, $J = 6.1$ Hz, 3H), 0.75 (d, $J = 6.1$ Hz, 3H), 0.71 (d, $J = 6.6$ Hz, 3H), 0.53 (d, $J = 6.6$ Hz, 3H); ^{13}C NMR (151 MHz, DMSO) δ 170.12, 167.31, 164.54, 159.31, 157.39, 153.63, 152.48, 150.58, 142.48, 141.55, 140.39, 138.16, 137.97, 135.06, 132.44, 131.34, 131.15, 130.93, 130.09, 129.35, 128.88, 126.59, 123.91, 122.83, 122.41, 120.25, 119.77, 119.73, 103.31, 61.72, 52.75, 47.01, 31.32, 28.61, 27.11, 24.59, 23.71, 23.60, 22.43, 22.24, 20.23, 19.50, 17.18, 14.33; IR (Neat) 3239, 2957, 2924, 2854,

1688, 1658, 1600, 1577, 1534, 1508, 1494, 1465, 1412, 1321, 1296, 1231, 1188, 1145, 1120, 1033, 842, 785, 738, 698, 659, 558, 464, 411 cm^{-1} ; HRMS (MM: ESI-APCI+) m/z calc'd for $\text{C}_{44}\text{H}_{48}\text{N}_9\text{O}_3$ $[\text{M} + \text{H}]^+$: 750.3880; found: 750.3883.

4.1.41. (S)-3-benzyl-5-methyl-N-(4-methyl-3-(1-methyl-7-((6-methylpyridin-3-yl)amino)-2-oxo-1,4-dihydropyrimido[4,5-d]pyrimidin-3(2H)-yl)phenyl)-2-oxo-2,3-dihydro-1H-benzo[e][1,4]diazepine-8-carboxamide (11k)

(Purity: 99%; HPLC); R_f : 0.35 (1:10 MeOH: CH_2Cl_2); $[\alpha]_{\text{D}}^{33} = +60.3$ (c 0.110, MeOH); ^1H NMR (600 MHz, DMSO) δ 10.66 (s, 1H), 10.44 (s, 1H), 9.66 (s, 1H), 8.81 (d, $J = 2.7$ Hz, 1H), 8.15 (d, $J = 3.0$ Hz, 1H), 8.06 (dd, $J = 8.5, 2.6$ Hz, 1H), 7.88–7.79 (m, 2H), 7.75–7.71 (m, 1H), 7.64 (s, 1H), 7.59 (d, $J = 8.2$ Hz, 1H), 7.29 (d, $J = 8.4$ Hz, 1H), 7.27–7.16 (m, 5H), 7.14 (t, $J = 7.3$ Hz, 1H), 4.70 (d, $J = 13.7$ Hz, 1H), 4.55–4.45 (m, 1H), 3.55 (d, $J = 14.0$ Hz, 1H), 3.44–3.40 (m, 1H), 3.34 (s, 3H), 3.16 (dt, $J = 15.0, 7.5$ Hz, 1H), 2.41 (s, 6H), 2.13 (s, 3H); ^{13}C NMR (151 MHz, DMSO) δ 169.93, 167.27, 164.76, 159.28, 157.37, 153.59, 152.45, 150.45, 141.52, 140.14, 139.58, 138.08, 137.61, 137.59, 135.14, 131.19, 131.12, 130.88, 129.90, 129.87, 129.14, 128.40, 126.75, 126.30, 122.93, 122.23, 120.87, 119.95, 119.42, 119.38, 103.34, 64.85, 46.99, 37.34, 28.61, 25.86, 23.49, 17.16; IR (Neat) 3278, 2923, 2853, 2360, 2340, 1669, 1600, 1534, 1496, 1411, 1296, 1236, 1189, 1145, 1113, 1072, 1029, 834, 786, 737, 700 cm^{-1} ; HRMS (MM: ESI-APCI+) m/z calc'd for $\text{C}_{38}\text{H}_{36}\text{N}_9\text{O}_3$ $[\text{M} + \text{H}]^+$: 666.2941; found: 666.2943.

4.1.42. (R)-3-benzyl-5-methyl-N-(4-methyl-3-(1-methyl-7-((6-methylpyridin-3-yl)amino)-2-oxo-1,4-dihydropyrimido[4,5-d]pyrimidin-3(2H)-yl)phenyl)-2-oxo-2,3-dihydro-1H-benzo[e][1,4]diazepine-8-carboxamide (11l)

(Purity: 98%; HPLC); R_f : 0.35 (1:10 MeOH: CH_2Cl_2); $[\alpha]_{\text{D}}^{25} = -73.5$ (c 0.0890, MeOH); ^1H NMR (600 MHz, DMSO) δ 10.66 (s, 1H), 10.44 (s, 1H), 9.66 (s, 1H), 8.81 (d, $J = 2.7$ Hz, 1H), 8.15 (d, $J = 3.0$ Hz, 1H), 8.06 (dd, $J = 8.5, 2.6$ Hz, 1H), 7.88–7.79 (m, 2H), 7.75–7.71 (m, 1H), 7.64 (s, 1H), 7.59 (d, $J = 8.2$ Hz, 1H), 7.29 (d, $J = 8.4$ Hz, 1H), 7.27–7.16 (m, 5H), 7.14 (t, $J = 7.3$ Hz, 1H), 4.70 (d, $J = 13.7$ Hz, 1H), 4.55–4.45 (m, 1H), 3.55 (d, $J = 14.0$ Hz, 1H), 3.44–3.40 (m, 1H), 3.34 (s, 3H), 3.16 (dt, $J = 15.0, 7.5$ Hz, 1H), 2.41 (s, 6H), 2.13 (s, 3H); ^{13}C NMR (151 MHz, DMSO) δ 169.93, 167.27, 164.76, 159.28, 157.37, 153.59, 152.45, 150.45, 141.52, 140.14, 139.58, 138.08, 137.61, 137.59, 135.14, 131.19, 131.12, 130.88, 129.90, 129.87, 129.14, 128.40, 126.75, 126.30, 122.93, 122.23, 120.87, 119.95, 119.42, 119.38, 103.34, 64.85, 46.99, 37.34, 28.61, 25.86, 23.49, 17.16; IR (Neat) 3279, 2921, 1668, 1598, 1531, 1494, 1408, 1239, 1186, 1143, 1112, 1071, 1026, 826, 785, 732, 698 cm^{-1} ; HRMS (MM: ESI-APCI+) m/z calc'd for $\text{C}_{38}\text{H}_{36}\text{N}_9\text{O}_3$ $[\text{M} + \text{H}]^+$: 666.2941; found: 666.2947.

4.1.43. (S)-3-isobutyl-1,5-dimethyl-N-(4-methyl-3-(1-methyl-7-((6-methylpyridin-3-yl)amino)-2-oxo-1,4-dihydropyrimido[4,5-d]pyrimidin-3(2H)-yl)phenyl)-2-oxo-2,3-dihydro-1H-benzo[e][1,4]diazepine-8-carboxamide (11m)

(Purity: 98%; HPLC); R_f : 0.35 (1:10 MeOH: CH_2Cl_2); $[\alpha]_{\text{D}}^{30} = +36.0$ (c 0.0500, MeOH); ^1H NMR (600 MHz, DMSO) δ 10.45 (s, 1H), 9.64 (s, 1H), 8.80 (d, $J = 2.7$ Hz, 1H), 8.16 (s, 1H), 8.05 (dd, $J = 8.5, 2.7$ Hz, 1H), 7.95 (s, 1H), 7.88 (d, $J = 8.1$ Hz, 1H), 7.85–7.77 (m, 2H), 7.68–7.61 (m, 1H), 7.32 (d, $J = 8.4$ Hz, 1H), 7.17 (d, $J = 8.4$ Hz, 1H), 4.70 (d, $J = 13.9$ Hz, 1H), 4.53 (d, $J = 14.0$ Hz, 1H), 3.40 (m, 1H), 3.36 (s, 3H), 3.34 (s, 3H), 2.43 (s, 3H), 2.40 (s, 3H), 2.14 (s, 3H), 1.93 (ddd,

$J = 13.5, 8.4, 5.2$ Hz, 1H), 1.72 (ddd, $J = 33.0, 13.6, 6.6, 6.1$ Hz, 2H), 0.85 (d, $J = 6.4$ Hz, 3H), 0.70 (d, $J = 6.3$ Hz, 3H); ^{13}C NMR (151 MHz, DMSO) δ 170.07, 167.18, 164.65, 159.31, 157.39, 153.61, 152.48, 150.57, 141.77, 141.54, 140.39, 138.00, 137.50, 135.06, 132.63, 131.27, 131.14, 128.14, 126.59, 123.59, 122.82, 121.23, 121.20, 120.14, 119.66, 103.31, 60.66, 47.00, 35.06, 28.61, 25.44, 24.23, 23.60, 23.58, 22.11, 17.17; IR (Neat) 3304, 2954, 1666, 1602, 1535, 1508, 1413, 1319, 1187, 1144, 1120, 1023, 827, 786, 746 cm^{-1} ; HRMS (MM: ESI-APCI+) m/z calc'd for $\text{C}_{36}\text{H}_{40}\text{N}_9\text{O}_3$ $[\text{M} + \text{H}]^+$: 646.3254; found: 646.3265.

4.1.44. (S)-3-isobutyl-1-(2-methoxyethyl)-N-(4-methyl-3-(1-methyl-7-((6-methylpyridin-3-yl)amino)-2-oxo-1,4-dihydropyrimido[4,5-d]pyrimidin-3(2H)-yl)phenyl)-2-oxo-5-phenyl-2,3-dihydro-1H-benzo[e][1,4]diazepine-8-carboxamide (11n)

(Purity: 98%; HPLC); R_f : 0.35 (1:10 MeOH: CH_2Cl_2); $[\alpha]_{\text{D}}^{23} = +20.3$ (c 0.0720, MeOH); ^1H NMR (600 MHz, DMSO) δ 10.51 (s, 1H), 9.65 (s, 1H), 8.80 (d, $J = 2.7$ Hz, 1H), 8.16 (d, $J = 2.8$ Hz, 2H), 8.05 (dd, $J = 8.5, 2.7$ Hz, 1H), 7.85–7.76 (m, 2H), 7.64 (dd, $J = 8.4, 2.2$ Hz, 1H), 7.55–7.50 (m, 3H), 7.49–7.44 (m, 2H), 7.39 (d, $J = 8.1$ Hz, 1H), 7.33 (d, $J = 8.4$ Hz, 1H), 7.18 (d, $J = 8.5$ Hz, 1H), 4.71 (d, $J = 14.0$ Hz, 1H), 4.54 (d, $J = 14.0$ Hz, 1H), 4.40 (dt, $J = 14.5, 5.6$ Hz, 1H), 3.99 (ddd, $J = 14.4, 6.5, 4.2$ Hz, 1H), 3.58 (dd, $J = 8.7, 4.5$ Hz, 1H), 3.42–3.35 (m, 2H), 3.34 (s, 3H), 2.95 (s, 3H), 2.41 (s, 3H), 2.14 (s, 3H), 2.11 (q, $J = 8.8$ Hz, 1H), 1.86–1.80 (m, 2H), 0.93 (d, $J = 5.9$ Hz, 3H), 0.76 (d, $J = 5.9$ Hz, 3H); ^{13}C NMR (151 MHz, DMSO) δ 169.32, 167.58, 164.67, 159.31, 157.39, 153.62, 152.48, 150.58, 142.78, 141.56, 140.39, 138.48, 138.04, 138.03, 137.81, 135.06, 132.37, 131.29, 131.16, 131.14, 130.78, 129.81, 129.42, 128.69, 126.59, 123.91, 122.86, 122.83, 120.16, 120.14, 119.64, 119.60, 103.31, 69.70, 61.57, 58.27, 47.01, 28.61, 24.63, 23.67, 23.60, 22.29, 17.18; IR (Neat) 3292, 2953, 2360, 1662, 1598, 1533, 1492, 1411, 1293, 1238, 1187, 1144, 1119, 1022, 909, 825, 784, 737, 697 cm^{-1} ; HRMS (MM: ESI-APCI+) m/z calc'd for $\text{C}_{43}\text{H}_{46}\text{N}_9\text{O}_4$ $[\text{M} + \text{H}]^+$: 752.3673; found: 752.3667.

4.1.45. (S)-1-(2-(benzylamino)-2-oxoethyl)-3-isobutyl-N-(4-methyl-3-(1-methyl-7-((6-methylpyridin-3-yl)amino)-2-oxo-1,4-dihydropyrimido[4,5-d]pyrimidin-3(2H)-yl)phenyl)-2-oxo-5-phenyl-2,3-dihydro-1H-benzo[e][1,4]diazepine-8-carboxamide (11o)

(Purity: 96%; HPLC); R_f : 0.35 (1:10 MeOH: CH_2Cl_2); $[\alpha]_{\text{D}}^{30} = +39.0$ (c 0.0670, MeOH); ^1H NMR (600 MHz, DMSO) δ 10.54 (s, 1H), 9.65 (s, 1H), 8.81 (d, $J = 2.8$ Hz, 1H), 8.67 (t, $J = 6.0$ Hz, 1H), 8.17 (s, 1H), 8.09–7.99 (m, 2H), 7.82 (q, $J = 2.4$ Hz, 1H), 7.80–7.77 (m, 1H), 7.63 (dd, $J = 8.1, 2.4$ Hz, 1H), 7.56–7.53 (m, 2H), 7.51 (t, $J = 7.3$ Hz, 1H), 7.45 (t, $J = 7.5$ Hz, 2H), 7.40 (d, $J = 8.1$ Hz, 1H), 7.34 (d, $J = 8.5$ Hz, 1H), 7.25 (dt, $J = 15.7, 7.6$ Hz, 4H), 7.18 (dd, $J = 8.1, 4.6$ Hz, 2H), 4.66 (dtd, $J = 46.8, 16.2, 15.1, 3.8$ Hz, 3H), 4.55 (d, $J = 14.0$ Hz, 1H), 4.34 (dd, $J = 15.4, 6.0$ Hz, 1H), 4.26 (dd, $J = 15.4, 5.7$ Hz, 1H), 3.66 (qd, $J = 4.5, 1.9$ Hz, 1H), 3.35 (s, 3H), 2.41 (s, 3H), 2.15 (s, 3H), 2.13 (d, $J = 8.8$ Hz, 1H), 1.90–1.82 (m, 2H), 0.95 (d, $J = 6.1$ Hz, 3H), 0.78 (d, $J = 5.9$ Hz, 3H); ^{13}C NMR (151 MHz, DMSO) δ 169.56, 167.99, 167.90, 164.84, 159.32, 157.39, 153.62, 152.49, 150.55, 143.08, 141.58, 140.35, 139.43, 138.73, 138.07, 138.05, 137.94, 135.08, 131.62, 131.32, 131.19, 130.70, 130.04, 129.66, 128.61, 128.59, 127.44, 127.08, 126.63, 123.43, 122.84, 122.13, 122.12, 120.09, 119.60, 119.56, 103.30, 63.16, 61.40, 50.68, 47.02, 42.48, 40.22, 28.61, 24.61, 23.73, 23.57, 22.25, 17.18; IR (Neat) 3294, 2953, 2360, 1661, 1597, 1531, 1409, 1292, 1233, 1187, 1144, 1119, 1028, 908, 826, 784, 736, 697 cm^{-1} ; HRMS (MM: ESI-APCI+) m/z calc'd for $\text{C}_{49}\text{H}_{49}\text{N}_{10}\text{O}_4$ $[\text{M} + \text{H}]^+$: 841.3938; found: 841.3947.

4.1.46. (S)-2-(5-(but-3-en-1-yl)-1-methyl-2-oxo-2,3-dihydro-1H-benz[e][1,4]diazepin-3-yl)-N-(4-methyl-3-(1-methyl-7-((6-methylpyridin-3-yl)amino)-2-oxo-1,4-dihydropyrimido[4,5-d]pyrimidin-3(2H)-yl)phenyl)acetamide (11p)

(Purity: 97%; HPLC); R_f : 0.35 (1:10 MeOH:CH₂Cl₂); $[\alpha]_D^{30} = -17.0$ (c 0.0780, MeOH); ¹H NMR (600 MHz, DMSO) δ 10.18 (s, 1H), 9.69 (s, 1H), 8.83 (s, 1H), 8.13 (s, 1H), 8.08 (d, $J=8.5$ Hz, 1H), 7.71 (d, $J=7.8$ Hz, 1H), 7.67 (d, $J=14.5$ Hz, 1H), 7.60 (t, $J=7.9$ Hz, 1H), 7.50 (d, $J=8.4$ Hz, 1H), 7.32 (t, $J=8.2$ Hz, 2H), 7.22 (dd, $J=14.1, 8.4$ Hz, 2H), 5.67 (dt, $J=16.6, 8.4$ Hz, 1H), 4.84 (d, $J=13.6$ Hz, 2H), 4.63 (d, $J=14.0$ Hz, 1H), 4.47 (d, $J=14.1$ Hz, 1H), 3.90 (d, $J=7.2$ Hz, 1H), 3.31 (s, 3H), 3.25 (s, 3H), 3.12 (td, $J=15.8, 6.9$ Hz, 1H), 2.97 (ddt, $J=30.1, 14.6, 7.4$ Hz, 2H), 2.75 (dt, $J=15.4, 7.9$ Hz, 1H), 2.42 (s, 3H), 2.21 (m, 1H), 2.14 (m, 1H), 2.08 (s, 3H); ¹³C NMR (151 MHz, DMSO) δ 170.61, 169.82, 169.67, 159.18, 157.39, 153.53, 152.39, 150.08, 142.17, 141.47, 138.45, 137.66, 131.59, 131.07, 130.00, 129.83, 127.62, 127.32, 124.88, 123.29, 122.25, 118.45, 118.04, 115.54, 103.48, 59.82, 46.92, 39.00, 36.78, 34.93, 31.22, 31.20, 28.58, 23.16, 18.45, 17.04; IR (Neat) 3305, 2924, 2361, 1666, 1601, 1535, 1493, 1413, 1293, 1235, 1194, 1144, 1117, 1025, 845, 750 cm⁻¹; HRMS (MM: ESI-APCI+) m/z calc'd for C₃₆H₃₈N₉O₃ [M + H]⁺: 644.3098; found: 644.3099.

4.1.47. (S)-2-(1-benzyl-5-(but-3-en-1-yl)-2-oxo-2,3-dihydro-1H-benz[e][1,4]diazepin-3-yl)-N-(4-methyl-3-(1-methyl-7-((6-methylpyridin-3-yl)amino)-2-oxo-1,4-dihydropyrimido[4,5-d]pyrimidin-3(2H)-yl)phenyl)acetamide (11q)

(Purity: 98%; HPLC); R_f : 0.35 (1:10 MeOH:CH₂Cl₂); $[\alpha]_D^{25} = +45.8$ (c 0.0610, MeOH); ¹H NMR (400 MHz, DMSO) δ 10.20 (s, 1H), 9.63 (s, 1H), 8.79 (d, $J=2.6$ Hz, 1H), 8.13 (d, $J=1.7$ Hz, 1H), 8.05 (dd, $J=8.4, 2.7$ Hz, 1H), 7.72–7.62 (m, 2H), 7.62–7.48 (m, 2H), 7.34 (td, $J=8.3, 2.2$ Hz, 1H), 7.27 (t, $J=7.4$ Hz, 1H), 7.24–7.13 (m, 5H), 7.03 (d, $J=7.3$ Hz, 2H), 5.79–5.66 (m, 1H), 5.33 (dd, $J=15.7, 3.8$ Hz, 1H), 4.97–4.85 (m, 3H), 4.63 (d, $J=14.1$ Hz, 1H), 4.48 (d, $J=14.1$ Hz, 1H), 4.02 (t, $J=7.1$ Hz, 1H), 3.34 (s, 3H), 3.22 (ddd, $J=16.8, 9.9, 7.4$ Hz, 1H), 3.10–2.99 (m, 1H), 2.79–2.70 (m, 2H), 2.40 (s, 3H), 2.09 (s, 3H), 1.98 (q, $J=7.5$ Hz, 2H); ¹³C NMR (101 MHz, DMSO) δ 170.79, 169.79, 169.35, 169.33, 159.41, 157.50, 153.66, 152.53, 150.67, 141.62, 140.53, 140.51, 138.54, 138.04, 137.62, 135.18, 131.66, 131.18, 131.14, 130.15, 128.79, 127.72, 127.61, 127.56, 126.69, 125.49, 122.98, 122.91, 118.63, 118.27, 115.55, 103.42, 59.96, 49.63, 47.06, 39.01, 36.96, 31.09, 31.07, 28.67, 23.70, 17.16; IR (Neat) 3300, 2923, 1667, 1599, 1534, 1491, 1449, 1409, 1330, 1290, 1236, 1186, 1143, 1116, 1079, 1024, 914, 826, 734, 699 cm⁻¹; HRMS (MM: ESI-APCI+) m/z calc'd for C₄₂H₄₂N₉O₃ [M + H]⁺: 720.3411; found: 720.3410.

4.2. Computational methods

For molecular modelling studies, crystal structures of Lck (PDB: 2PLO), c-Src (PDB: 3OEZ), p38a (PDB: 3HEC) and Abl1 (PDB: 2HYY) were downloaded from the RCSB protein data bank homepage (<https://www.rcsb.org>). Only the crystal structures bound with Imatinib were selected to obtain the DFG-out state of kinases. The chicken c-Src crystal structure was converted into a human c-Src structure using a homology modelling method. The missing activation loop in p38a crystal structure was restored based on the crystal structure of Lck using Prime loop prediction application¹⁷. For protein-ligand complex prediction, Glide docking application¹⁸ in Schrödinger suite was employed. OPLS3e force field and SP mode of Glide were used. Flexible ligand sampling was allowed. Molecular dynamics simulation was performed using Desmond

molecular dynamics package¹⁹ in Schrödinger suite. The kinase-inhibitor complexes were solvated using TIP3P water model and the solvated MD systems were described using OPLS3e force field. The Nose-Hoover chain thermostat and the Martyna-Tobias-Klein barostat methods were used to maintain the system temperature at 300 K and system pressure at 1 bar, respectively. A periodic boundary condition was employed. MD simulations were performed for 3 μ s simulation time. Binding free energies of inhibitors were calculated by Prime molecular mechanics/generalized Born surface area (MM/GBSA) application with VSGB2.0 implicit solvation model. WaterMap²⁰ application in Schrödinger suites was used.

4.3. Biology

4.3.1. In vitro kinase assay

Full panel kinase profiling and kinase IC₅₀ measurement were performed by using Reaction Biology Corp. (San Diego, USA).

4.3.2. Cell culture and sample treatment

Jurkat cells were purchased from the Korea Cell Line Bank (Seoul, Republic of Korea) and maintained in RPMI-1640 medium containing 10% FBS, streptomycin sulphate, penicillin, HEPES, and sodium bicarbonate in a 5% CO₂ atmosphere at 37 °C. Jurkat cells were stimulated with 1 μ g/ml of plate-bound anti-CD3 mAb (clone HIT3a, BD Bioscience) and then incubated with KITS 1-001 (10, 50, or 100 μ M) for 30 min. KITS 1-001 were dissolved in DMSO and added to the culture media in serial dilution (the final concentration of DMSO in all experiments did not exceed 0.1%).

4.3.3. Western blot analysis

The protein of Jurkat cells was extracted using a PRO-PREP (Intron Biotechnology, Seoul, Republic of Korea). The protein concentration was determined using Bio-Rad protein assay reagent according to the manufacturer's instruction and BSA (Bio-Rad, Hercules, CA, USA) was used as a standard for quantification. Equal protein amounts were separated by 10% sodium dodecyl sulphate-polyacrylamide gel electrophoresis (SDS-PAGE) and transferred to PVDF membranes. The membranes were incubated for 1 h with blocking solution (5% skim milk) at room temperature and followed by incubation for primary antibodies overnight at 4 °C. p-Lck (Y394) antibody (1:500, MBS128234, MyBioSource) was used as a primary antibody, and β -actin (1:1000, sc-81178, Santa Cruz Biotechnology) was used as an internal control. And then membranes were incubated with a 1:2000 dilution of horseradish peroxidase-conjugated secondary antibody for 2 h at room temperature. The membranes were analysed using an enhanced chemiluminescence (ECL) substrate and imaged by LAS-4000 luminescent image analyser (FUJIFILM, Tokyo, Japan).

4.3.4. Animals

Male C57BL/6 mice (21 \pm 2 g; 6 weeks) were obtained from Oriental Bio Inc. (Seongnam-si, Korea). All mice were bred under constant conditions (temperature: 22 \pm 2 °C, humidity: 40–60%, light/dark cycle: 12 h). All animal experiments were conducted under the university guidelines of the ethical committee for Animal Care and Use of the Kyung Hee University (KHSASP-22-002).

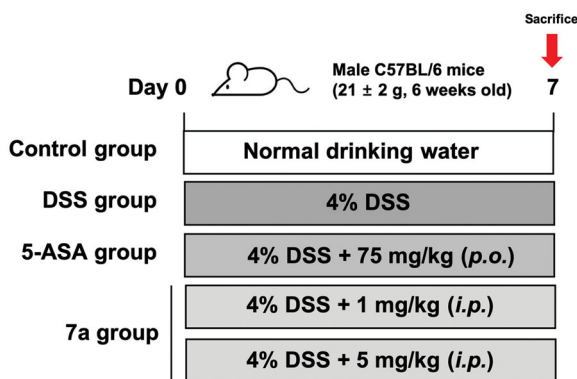


Figure 8. Schematic diagram of DSS-induced colitis mouse model.

4.3.5. Induction of colitis by dextran sulphate sodium (DSS) and treatment

Colitis in mice was induced by providing water containing 4% (w/v) DSS for 7 days. Mice were randomly divided into 5 groups ($n=6/\text{group}$, Figure 8) as follows: control group treated with vehicle; DSS plus vehicle group exposed to 4% DSS and treated with vehicle; the other 3 groups consist of mice receiving 4% DSS was treated with 5-ASA (75 mg/kg/day, *p.o.*) as a positive control or **7a** (1, 5 mg/kg/day, *i.p.*) daily for 7 days.

4.3.6. Assessment of the disease activity index (DAI)

To calculate the severity of colitis, body weight, stool consistency, and occult/gross bleeding of all mice were assessed. DAI score was measured every day according to the following table (Table 5). The colon length was measured at end of the experiment.

4.3.7. Statistical analysis

Results are expressed as the mean \pm SE of triplicate experiments with similar patterns. Statistically significant values were compared using ANOVA and Dunnett's *post hoc* test, and *p* values of less than 0.05 were considered statistically significant.

Disclosure statement

No potential conflict of interest was reported by the author(s).

Funding

This work was supported by Korea Institute of Science and Technology (KIST), the National Research Foundation of Korea (NRF) funded by the Korean government (MEST) [2017R1A2B3006704, 2019R1A6A1A03032869, NRF2016M3A9B5940991, NRF-2021R1A2C3011992], the Brain Korea 21 FOUR Project for Medical Science in Yonsei University College of Medicine, and the Technology Development Program to Solve Climate Change of the National Research Foundation (NRF) of Korea funded by the Ministry of Science and ICT (NRF-2020M1A2A2079798). This research was supported by the National Research Council of Science & Technology (NST) granted by the Korea government (MSIT) (No. CPS21061-100).

ORCID

Seo-Jung Han <http://orcid.org/0000-0002-5812-3826>

In Ho Park <http://orcid.org/0000-0003-2190-5469>

Jeon-Soo Shin <http://orcid.org/0000-0002-8294-3234>

References

- For selected reviews, see: (a) Wu P, Nielsen TE, Clausen MH. Small-molecule kinase inhibitors: an analysis of FDA-approved drugs. *Drug Discovery Today* 2016;21:5–10. (b) Wu P, Nielsen TE, Clausen MH. FDA-approved small-molecule kinase inhibitors. *Trends Pharmacol Sci* 2015;36:422–39. (c) Zhang J, Yang PL, Gray NS. Targeting cancer with small molecule kinase inhibitors. *Nat Rev Cancer* 2009;9:28–39. (d) Ferguson FM, Gray NS. Kinase inhibitors: the road ahead. *Nat Rev Drug Discov* 2018;17:353–77. (e) Fedorov O, Müller S, Knapp S. The (un)targeted cancer kinome. *Nat Chem Biol* 2010;6:166–9. (f) Schwartz PA, Murray BW. Protein kinase biochemistry and drug discovery. *Bioorg Chem* 2011;39:192–210. (g) Cohen P. Protein kinases—the major drug targets of the twenty-first century? *Nat Rev Drug Discov* 2002;1:309–15. (h) Grant SK. Therapeutic protein kinase inhibitors. *Cell Mol Life Sci* 2009;66:1163–77. (i) Pottier C, Fresnais M, Gilon M, et al. Tyrosine kinase inhibitors in cancer: breakthrough and challenges of targeted therapy. *Cancers* 2020;12:731. (j) Gagic Z, Ruzic D, Djokovic N, et al. In silico methods for design of kinase inhibitors as anticancer drugs. *Frontiers in Chemistry* 2019;7:873.
- (a) Zhao Z, Wu H, Wang L, et al. Exploration of type II binding mode: a privileged approach for kinase inhibitor focused drug discovery? *ACS Chem Biol* 2014;9:1230–41. (b) Roskoski R., Jr. Classification of small molecule protein kinase inhibitors based upon the structures of their drug-enzyme complexes. *Pharmacol Res* 2016;103:26–48.
- (a) Sun J, Niu Y, Wang C, et al. Discovery of 3-benzyl-1,3-benzoxazine-2,4-dione analogues as allosteric mitogen-activated kinase kinase (MEK) inhibitors and anti-enterovirus 71 (EV71) agents. *Bioorg Med Chem* 2016;24:3472–82. (b) Comess KM, Sun C, Abad-Zapatero C, et al. Discovery and characterization of non-ATP site inhibitors of the mitogen activated protein (MAP) kinases. *ACS Chem Biol* 2011;6:234–44. (c) Wu P, Clausen MH, Nielsen TE. Allosteric small-molecule kinase inhibitors. *Pharmacol Therapeut* 2015;156:59–68. (d) Converso A, Hartingh T, Garbaccio RM, Tasber E, et al. Development of thioquinazolinones, allosteric Chk1 kinase inhibitors. *Bioorg Med Chem Lett* 2009;19:1240–4. (e) Lu X, Smaill JB, Ding K. New promise and opportunities for allosteric kinase inhibitors. *Angew Chem Int Ed Engl* 2020;59:13764–76.
- (a) Zhao Z, Bourne PE. Progress with covalent small-molecule kinase inhibitors. *Drug Discovery Today* 2018;23:727–35. (b) Liu Q, Sabnis Y, Zhao Z, et al. Developing irreversible inhibitors of the protein kinase cysteinome. *Chem Biol* 2013;20:146–59. (c) Weisner J, Gontla R, van der Westhuizen L, et al. Covalent-allosteric kinase inhibitors. *Angew Chem Int Ed Engl* 2015;54:10313–6. (d) Abdeldayem A, Raouf YS, Constantinescu SN, et al. Advances in covalent kinase inhibitors. *Chem Soc Rev* 2020;49:2617–87.
- (a) Norman RA, Toader D, Ferguson AD. Structural approaches to obtain kinase selectivity. *Trends Pharmacol Sci* 2012;33:273–8. (b) Davies SP, Reddy H, Caivano M, Cohen P. Specificity and mechanism of action of some commonly used protein kinase inhibitors. *Biochem J* 2000;351:95–105. (c) Müller S, Chaikuad A, Gray NS, Knapp S. The ins

- and outs of selective kinase inhibitor development. *Nat Chem Biol* 2015;11:818–21.
6. Liu Y, Han SJ, Liu WB, Stoltz BM. Catalytic enantioselective construction of quaternary stereocenters: assembly of key building blocks for the synthesis of biologically active molecules. *Acc Chem Res* 2015;48:740–51.
 7. (a) Zask A, Murphy J, Ellestad GA. Biological stereoselectivity of atropisomeric natural products and drugs. *Chirality* 2013; 25:265–74. (b) Porter J, Payne A, Whitcombe I, et al. Atropisomeric small molecule Bcl-2 ligands: Determination of bioactive conformation. *Bioorg Med Chem Lett* 2009;19: 1767–72. (c) Xing L, Devadas B, Devraj RV, et al. Discovery and characterization of atropisomer PH-797804, a p38 MAP kinase inhibitor, as a clinical drug candidate. *ChemMedChem* 2012;7:273–80. (d) Smith DE, Marquez I, Lokensgard ME, et al. Exploiting atropisomerism to increase the target selectivity of kinase inhibitors. *Angew Chem Int Ed Engl* 2015;54:11754–9.
 8. (a) Jiang J, Shen M, Thomas CJ, Boxer MB. Chiral kinase inhibitors. *Curr Top Med Chem* 2011;11:800–9. (b) Norman P. Evaluation of WO2011134971, chiral 1,6-naphthyridine Syk kinase inhibitors. *Expert Opin Ther Patents* 2012;22:335–9. (c) Kitano Y, Suzuki T, Kawahara E, Yamazaki T. Synthesis and inhibitory activity of 4-alkynyl and 4-alkenylquinazolines: Identification of new scaffolds for potent EGFR tyrosine kinase inhibitors. *Bioorg Med Chem Lett* 2007;17:5863–7. (d) Bühler S, Goettert M, Schollmeyer D, et al. Chiral sulfoxides as metabolites of 2-thioimidazole-based p38 α mitogen-activated protein kinase inhibitors: enantioselective synthesis and biological evaluation. *J Med Chem* 2011;54:3283–97. (e) Wu CH, Coumar MS, Chu CY, et al. Design and synthesis of tetrahydropyridothieno[2,3-d]pyrimidine scaffold based epidermal growth factor receptor (EGFR) kinase inhibitors: The role of side chain chirality and michael acceptor group for maximal potency. *J Med Chem* 2010;53:7316–26.
 9. (a) Choi HG, Ren P, Adrian F, et al. A type-II kinase inhibitor capable of inhibiting the T315I “gatekeeper” mutant of Bcr-Abl. *J Med Chem* 2010;53:5439–48. (b) Nonami A, Sattler M, Weisberg E, et al. Identification of novel therapeutic targets in acute leukemias with NRAS mutations using a pharmacologic approach. *Blood* 2015;125:3133–43. (c) Cho H, Shin I, Ju E, et al. First SAR study for overriding NRAS mutant driven acute myeloid leukemia. *J Med Chem* 2018;61: 8353–73.
 10. (a) Whitby LR, Ando Y, Setola V, et al. Design, Synthesis, and validation of a β -turn mimetic library targeting protein-protein and peptide-receptor interactions. *J Am Chem Soc* 2011;133:10184–94. (b) Metrano AJ, Abascal NC, Mercado BQ, et al. Diversity of secondary structure in catalytic peptides with β -turn-biased sequences. *J Am Chem Soc* 2017;139: 492–516. (c) Hata M, Marshall GR. Do benzodiazepines mimic reverse-turn structures? *J Comput Aided Mol Des* 2006;20:321–31. (d) Chauhan J, Chen SE, Fenstermacher KJ, et al. Synthetic, structural mimetics of the β -hairpin flap of HIV-1 protease inhibit enzyme function. *Bioorg Med Chem* 2015;23:7095–109. (e) Dörr AA, Lubell W. γ -Turn γ -Turn Mimicry with Benzodiazepinones and pyrrolbenzodiazepinones synthesized from a Common Amino ketone intermediate. *Org Lett* 2015;17:3592–5. (f) Peris G, Jakobsche CE, Miller SJ. Aspartate-catalyzed asymmetric epoxidation reactions. *J Am Chem Soc* 2007; 129:8710–1. (g) Lenci E, Trabocchi A. Peptidomimetic toolbox for drug discovery. *Chem Soc Rev* 2020;49:3262–77.
 11. WaterMap finds the hydration sites in the binding site using MD simulation and calculates the enthalpy and entropy energies of each the hydration site.
 12. (a) Spyraakis F, Ahmed MH, Bayden AS, et al. The roles of water in the protein matrix: a largely untapped resource for drug discovery. *J Med Chem* 2017;60:6781–827. (b) Robinson DD, Sherman W, Farid R. Understanding kinase selectivity through energetic analysis of binding site waters. *ChemMedChem* 2010;5:618–27. (c) Wang Y, Fu Q, Zhou Y, et al. Replacement of protein binding-site waters contributes to favorable halogen bond interactions. *J Chem Inf Model* 2019;59:3136–43. (d) Cappel D, Sherman W, Beuming T. Calculating water thermodynamics in the binding site of Proteins - Applications of WaterMap to Drug Discovery. *Curr Top Med Chem* 2017;17:2586–98. (e) Breiten B, Lockett MR, Sherman W, et al. Water networks contribute to enthalpy/entropy compensation in protein-ligand binding. *J Am Chem Soc* 2013;135:15579–84.
 13. Ananthakrishnan AN, Kaplan GG, Ng SC. Changing global epidemiology of inflammatory bowel diseases: sustaining health care delivery into the 21st Century. *Clin Gastroenterol Hepatol* 2020;18:1252–60.
 14. Giuffrida P, Sabatino AD. Targeting T cells in inflammatory bowel disease. *Pharmacol Res* 2020;159:105040.
 15. Singh PK, Kashyap A, Silakari O. Exploration of the therapeutic aspects of Lck: a kinase target in inflammatory mediated pathological conditions. *Biomed Pharmacother* 2018; 108:1565–71.
 16. Rose WA, Sakamoto K, Leifer CA. Multifunctional role of dextran sulfate sodium for *in vivo* modeling of intestinal diseases. *BMC Immunology* 2012;13:41.
 17. Schrödinger Release 2019-4: Prime. Schrödinger. New York, NY: LLC; 2019.
 18. Schrödinger Release 2019-4: Glide. Schrödinger. New York, NY: LLC; 2019.
 19. Schrödinger Release 2019-4: Desmond, Desmond Molecular Dynamics System, D. E. Shaw Research, New York, NY, 2020. Maestro-Desmond Interoperability Tools, Schrödinger, LLC, New York, NY, 2019.
 20. Schrödinger Release 2019-4: WaterMap. Schrödinger. New York, NY: LLC; 2019.